

ARGENTINE REPUBLIC
INVESTIGATION ON THE NOVELTY VALUE
OF THE MARK OF THE CHILAN VINO

REPORT OF THE
COMMISSION OF THE MARK

NOV 1968

INVESTIGATION ON THE NOVELTY VALUE

JICA
701
643
MPN
LIBRARY

643-03
643-03
643-03

ARGENTINE REPUBLIC
INTERIM REPORT ON THE NORTHERN NEUQUEN
GEOTHERMAL DEVELOPMENT PROJECT

FIRST•SECOND PHASE SURVEY
(SEPARATE VOLUME: FIGURES)

NOVEMBER 1983

JAPAN INTERNATIONAL COOPERATION AGENCY

JICA LIBRARY



1053759[5]

国際協力事業団	
受入 月日 '84.11.16	701
	64.3
登録No. 10846	MPN

マイクロ
フィニユ作成

List of Figures

- Fig. 1-1 Location map of the survey areas
- Fig. 1-2 Explanatory map of northern parts of the Province of Neuquen
- Fig. 2-1 Geological interpretation map of Landsat image
- Fig. 2-2 Regional geological map
- Fig. 2-3 Geological interpretation map of aerial photographs
- Fig. 2-4 Map of the survey areas and routes of reconnaissance geological survey
- Fig. 2-5 Schematic profile of geology and geothermal system
- Fig. 3-1 Principal points of aerial photographs and topographic standard points
- Fig. 3-2 Bird's-eye view map of the survey area
- Fig. 3-3 Geological columnar section of the survey area
- Fig. 3-4 Geological map of the survey area
- Fig. 3-5 Geological cross-sections
- Fig. 3-6 Modal diagram of quartz - potash feldspar - plagioclase
- Fig. 3-7 Rose diagram of joints in granodiorite
- Fig. 3-8 Alkali - silica diagram of younger volcanic rocks
- Fig. 3-9 MgO - total FeO - ($\text{Na}_2\text{O} + \text{K}_2\text{O}$) diagram of younger volcanic rocks
- Fig. 3-10 Location map of rock sampling
- Fig. 3-11 Physical properties of rocks
- Fig. 4-1 LaCoste & Romberg gravity meter Model - G
- Fig. 4-2 Sketches of reference station(a) and base station(b)
- Fig. 4-3 Network of leveling
- Fig. 4-4 Observations of diurnal gravity variation
- Fig. 4-5 Relation between gravity and altitude
- Fig. 4-6 Regional Bouguer anomaly map ($\rho = 2.30 \text{ g/cm}^3$)
- Fig. 4-7 Bouguer anomaly map ($\rho = 2.30 \text{ g/cm}^3$)

- Fig. 4-8 Bouguer anomaly map ($\rho = 2.00 \text{ g/cm}^3$)
- Fig. 4-9 Bouguer anomaly map ($\rho = 2.50 \text{ g/cm}^3$)
- Fig. 4-10 Long-wave Bouguer anomaly map ($\rho = 2.30 \text{ g/cm}^3$)
- Fig. 4-11 Short-wave Bouguer anomaly map ($\rho = 2.30 \text{ g/cm}^3$)
- Fig. 4-12 Three-dimensional image of Bouguer anomaly map ($\rho = 2.30 \text{ g/cm}^3$)
- Fig. 4-13 Zoning of Bouguer anomaly map
- Fig. 4-14 Gravimetric interpretation map
- Fig. 4-15 Analytical result of gravimetric cross-section along A - A' line
- Fig. 4-16 Analytical result of gravimetric cross-section along B - B' line
- Fig. 4-17 Analytical result of gravimetric cross-section along C - C' line
- Fig. 5-1 Location map of alteration zones
- Fig. 5-2 Sketched areas of alteration zone and regional distributions of alteration minerals
- Fig. 5-3 Sketch of alteration zone and diagrams of alternation minerals (1) Rincon de las Papas
- Fig. 5-4 Sketch of alteration zone and diagrams of alteration minerals (2) La Bramadora
- Fig. 5-5 Sketch of alteration zone and diagrams of alteration minerals (3) El Humazo - 1
- Fig. 5-6 Sketch of alteration zone and diagrams of alteration minerals (4) El Humazo - 2
- Fig. 5-7 Sketch of alteration zone and diagrams of alteration minerals (5) El Humazo - 3
- Fig. 5-8 Sketch of alteration zone and diagrams of alteration minerals (6) Las Olletas
- Fig. 5-9 Sketch of alteration zone and diagrams of alteration minerals (7) Los Tachos - 1
- Fig. 5-10 Sketch of alteration zone and diagrams of alteration minerals (8) Los Tachos - 2
- Fig. 5-11 Sketch of alteration zone and diagrams of alteration minerals (9) Los Tachos - 3

- Fig. 5-12 Typical charts of X-ray diffraction analysis
- Fig. 5-13 Alteration zoning map of Los Tachos - 3
- Fig. 5-14 Location map of test holes at 1 meter depth
- Fig. 5-15 Distribution map of ground temperature at 1 meter depth
- Fig. 5-16 Frequency distribution of ground temperature at 1 meter depth
- Fig. 5-17 Diurnal variation of atmospheric and ground temperatures
- Fig. 5-18 Observational results of variation of atmospheric and ground temperatures during period of 1 meter depth survey
- Fig. 5-19 Distribution map of ground temperature at 1 meter depth by running average method
- Fig. 5-20 Relation between altitude and ground temperature at 1 meter depth
- Fig. 5-21 Distribution map of residual ground temperature at 1 meter depth (calculated by linear equation)
- Fig. 5-22 Distribution map of residual ground temperature at 1 meter depth (calculated by quadratic equation)
- Fig. 5-23 Distribution map of Hg - concentration in soil
- Fig. 5-24 Frequency distribution of Hg - concentration in soil
- Fig. 5-25 Distribution map of Hg - concentration in soil by running average method
- Fig. 5-26 Distribution map of CO₂ - concentration in soil-air
- Fig. 5-27 Frequency distribution of CO₂ - concentration in soil-air
- Fig. 5-28 Distribution map of CO₂ - concentration in soil-air by running average method
- Fig. 5-29 Correlations between ground temperature, and Hg and CO₂ - concentrations
- Fig. 5-30 Correlations between residual ground temperature, and CO₂ - concentration(1) and Hg - concentration(2)
- Fig. 5-31 Relation map of anomalous values at 1 meter depth survey

- Fig. 5-32 Composite map of anomalous areas of ground temperature and Hg - CO₂ geochemistry
- Fig. 6-1 Location map of measurements of water discharge and calculations of specific rate of flow
- Fig. 6-2 Daily variations of discharge, water temperature and atmospheric temperature
- Fig. 6-3 Schematic columnar section of effective porosity
- Fig. 6-4 Location map of hot water, fumarolic gas and condensed water samplings
- Fig. 6-5 Detailed sketch of geothermal manifestation (1) Rincon de Las Papas
- Fig. 6-6 Detailed sketch of geothermal manifestation (2) La Bramadora
- Fig. 6-7 Detailed sketch of geothermal manifestation (3) El Humazo - 1
- Fig. 6-8 Detailed sketch of geothermal manifestation (4) El Humazo - 2
- Fig. 6-9 Detailed sketch of geothermal manifestation (5) El Humazo - 3
- Fig. 6-10 Detailed sketch of geothermal manifestation (6) Las Olletas
- Fig. 6-11 Detailed sketch of geothermal manifestation (7) Aguas Calientes
- Fig. 6-12 Detailed sketch of geothermal manifestation (8) Baños del Agua Caliente
- Fig. 6-13 Detailed sketch of geothermal manifestation (9) Los Tachos - 1
- Fig. 6-14 Detailed sketch of geothermal manifestation (10) Los Tachos - 2
- Fig. 6-15 Detailed sketch of geothermal manifestation (11) Los Tachos - 3
- Fig. 6-16 Main chemical compositions of hot water
- Fig. 6-17 (1) Hexadiagrams of main chemical compositions of hot water
- Fig. 6-17 (2) Hexadiagrams of main chemical compositions of hot water

- Fig. 6-17 (3) Hexadiagrams of main chemical compositions of hot water
- Fig. 6-18 Diagram of Cl - HCO₃ - B contents of hot water
- Fig. 6-19 Comparative diagrams of ion - concentration index between sea water and hot water
- Fig. 6-20 Silica - geochemical geothermometer
- Fig. 6-21 Silica - geochemical geothermometer (mixing model 1 - 1)
- Fig. 6-22 Silica - geochemical geothermometer (mixing model 1 - 2)
- Fig. 6-23 Silica - geochemical geothermometer (mixing model 2)
- Fig. 6-24 Composite map of zoning of hot spring - fumarole and geochemical geothermo-temperature
- Fig. 7-1 Synthetic interpretation map of geologic structure
- Fig. 7-2 Synthetic interpretation map of heat flow structure
- Fig. 7-3 Model of circulation mechanism of geothermal fluid and geothermal reservoir structure (1)
- Fig. 7-4 Model of circulation mechanism of geothermal fluid and geothermal reservoir structure (2)
- Fig. 8-1 Proposed working plan of the third phase survey

1. General Remarks

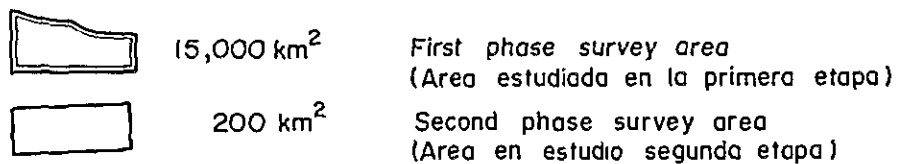
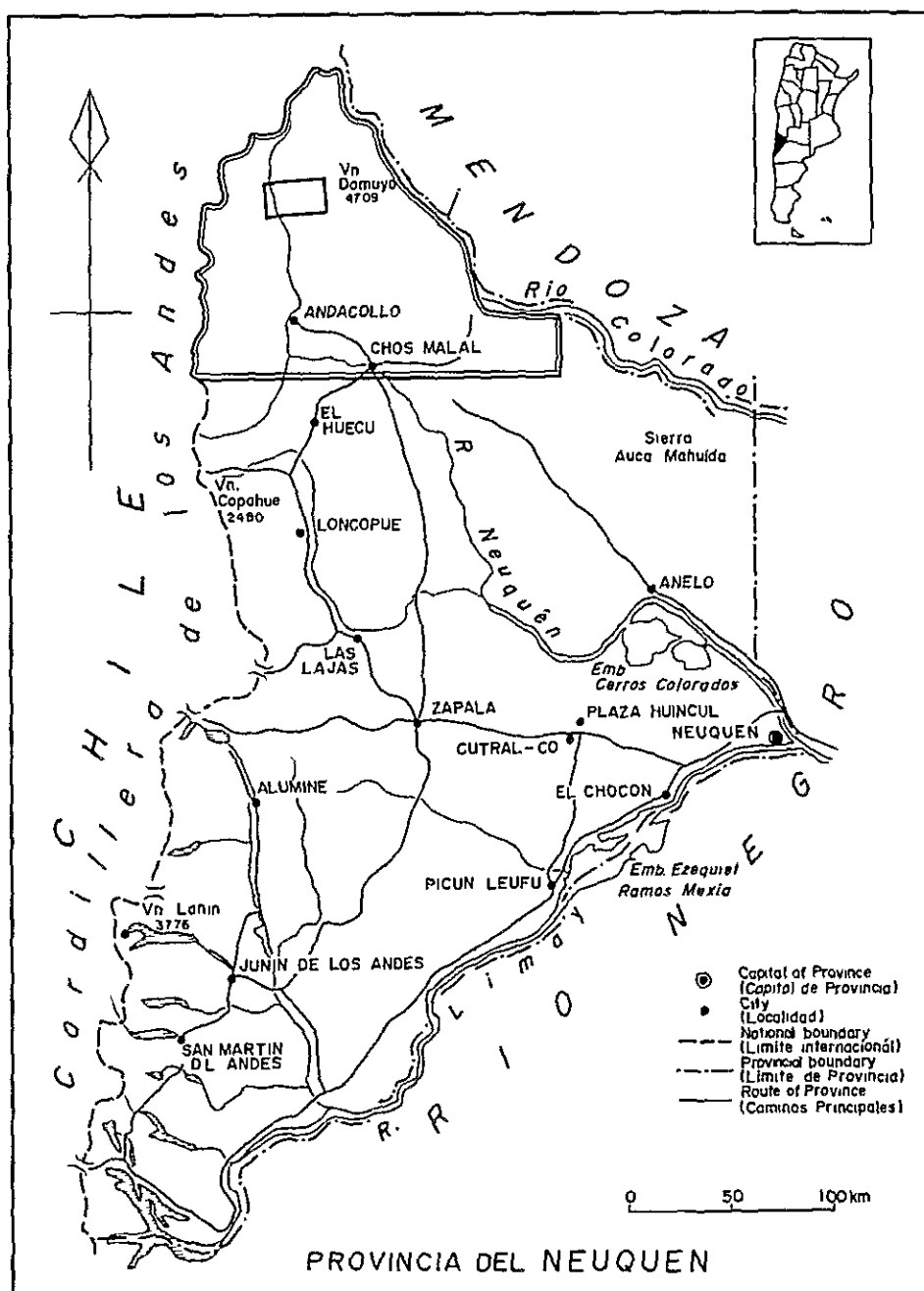


Fig.1-1 Location map of the survey areas

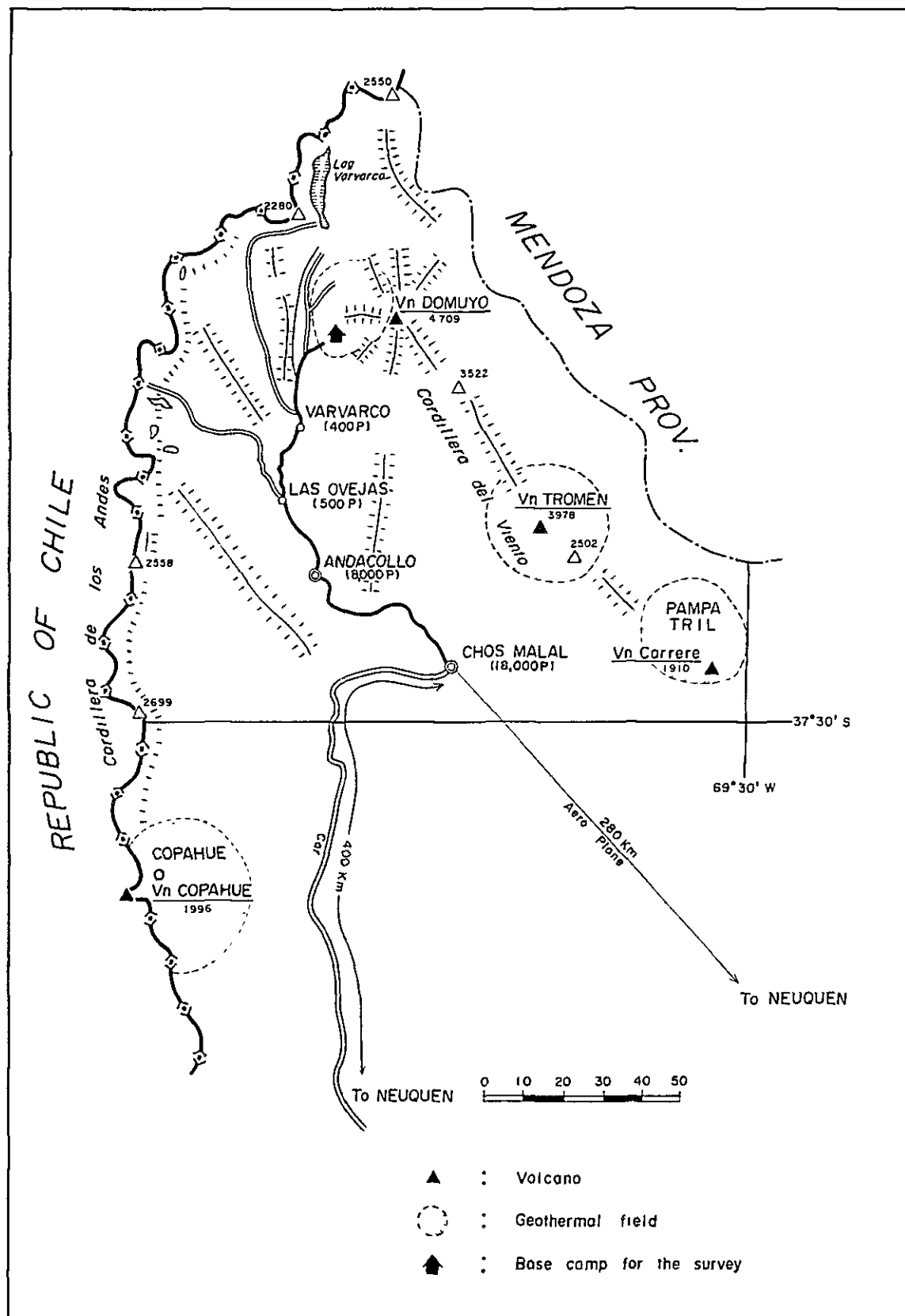
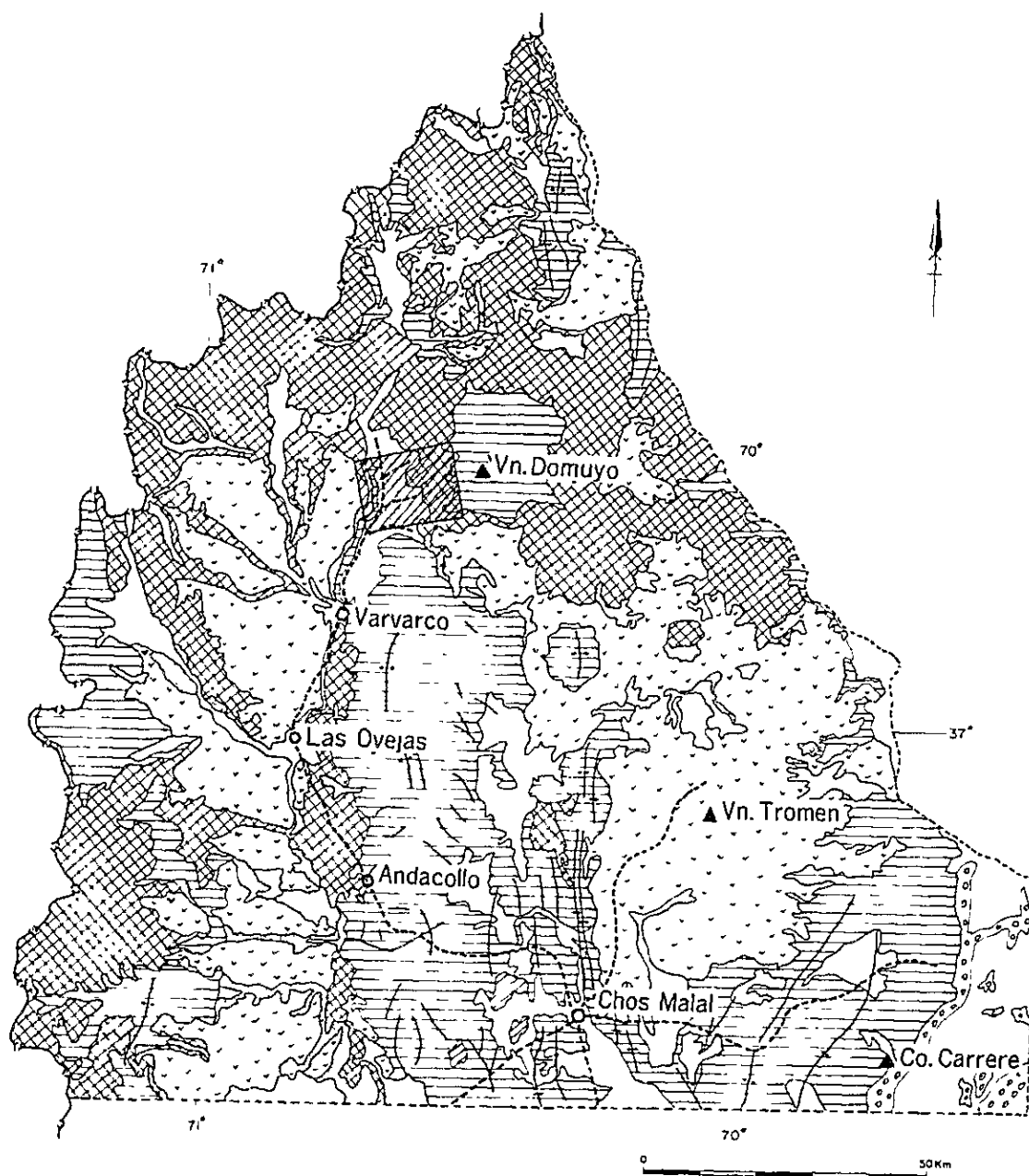


Fig.1-2 Explanatory map of northern parts of the Province of Neuquen

2. Outlines of the First Phase Survey



REGEND

Quaternary		Alluvium		Folding axes
		Andesite, Basalt		Road
Tertiary		Andesite, Basalt, Rhyolite		Selected area 200 Km²
		Andesite (volcanics, pyroclastics)		Village
		Andesite, Dacite		
pre-Tertiary		Basement		

Fig.2-1 Geological interpretation map of Landsat image

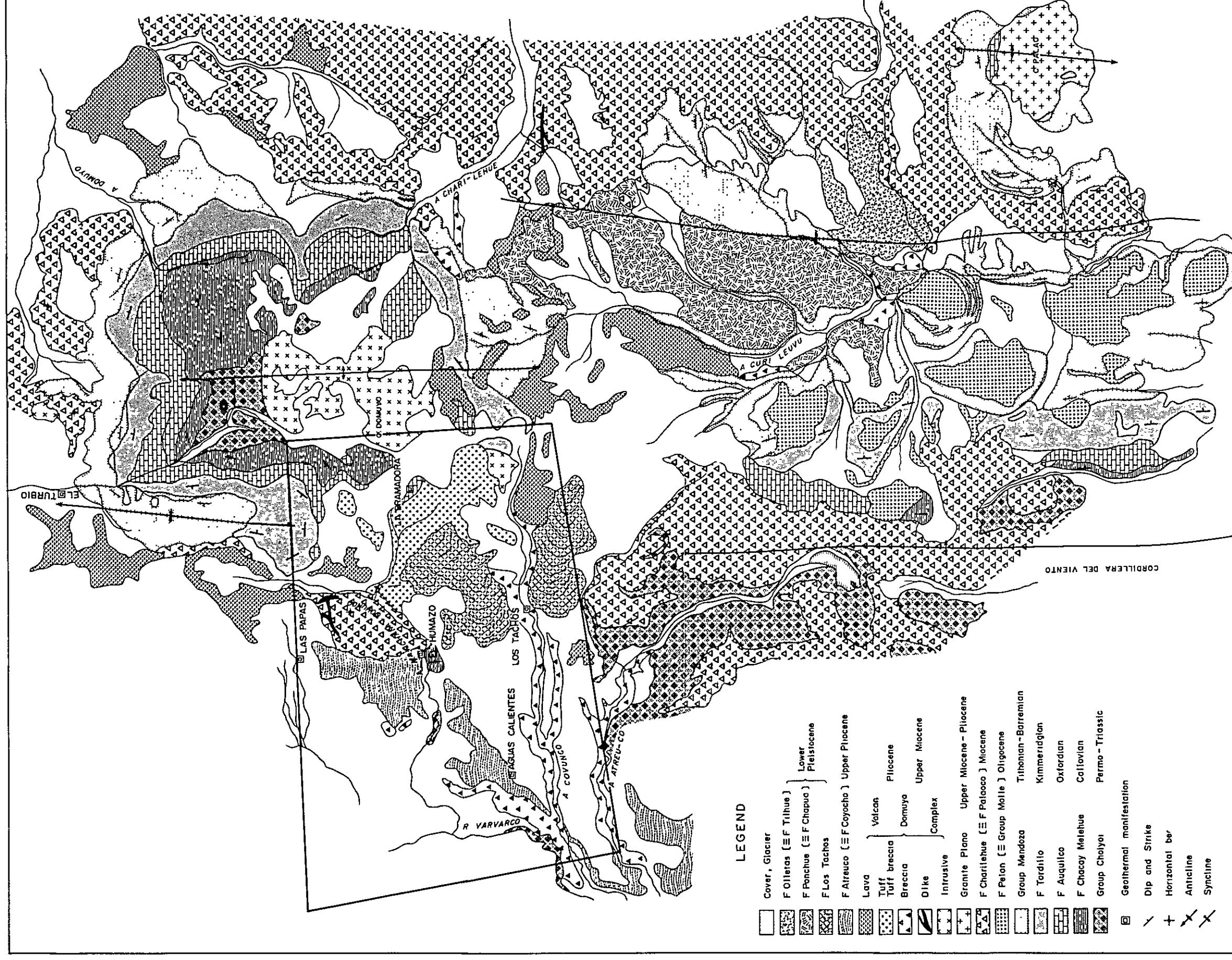


Fig.2-2 Regional geological map

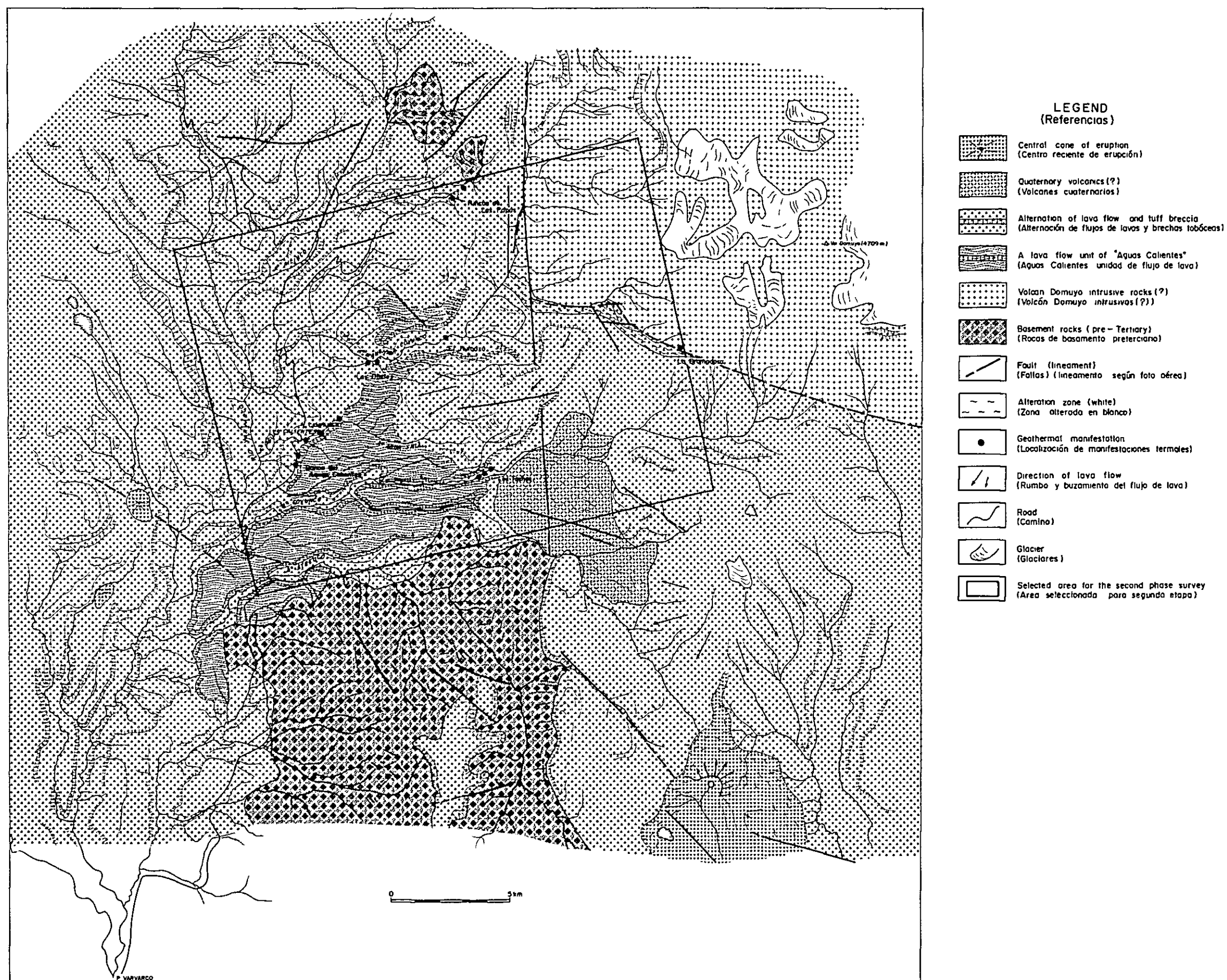
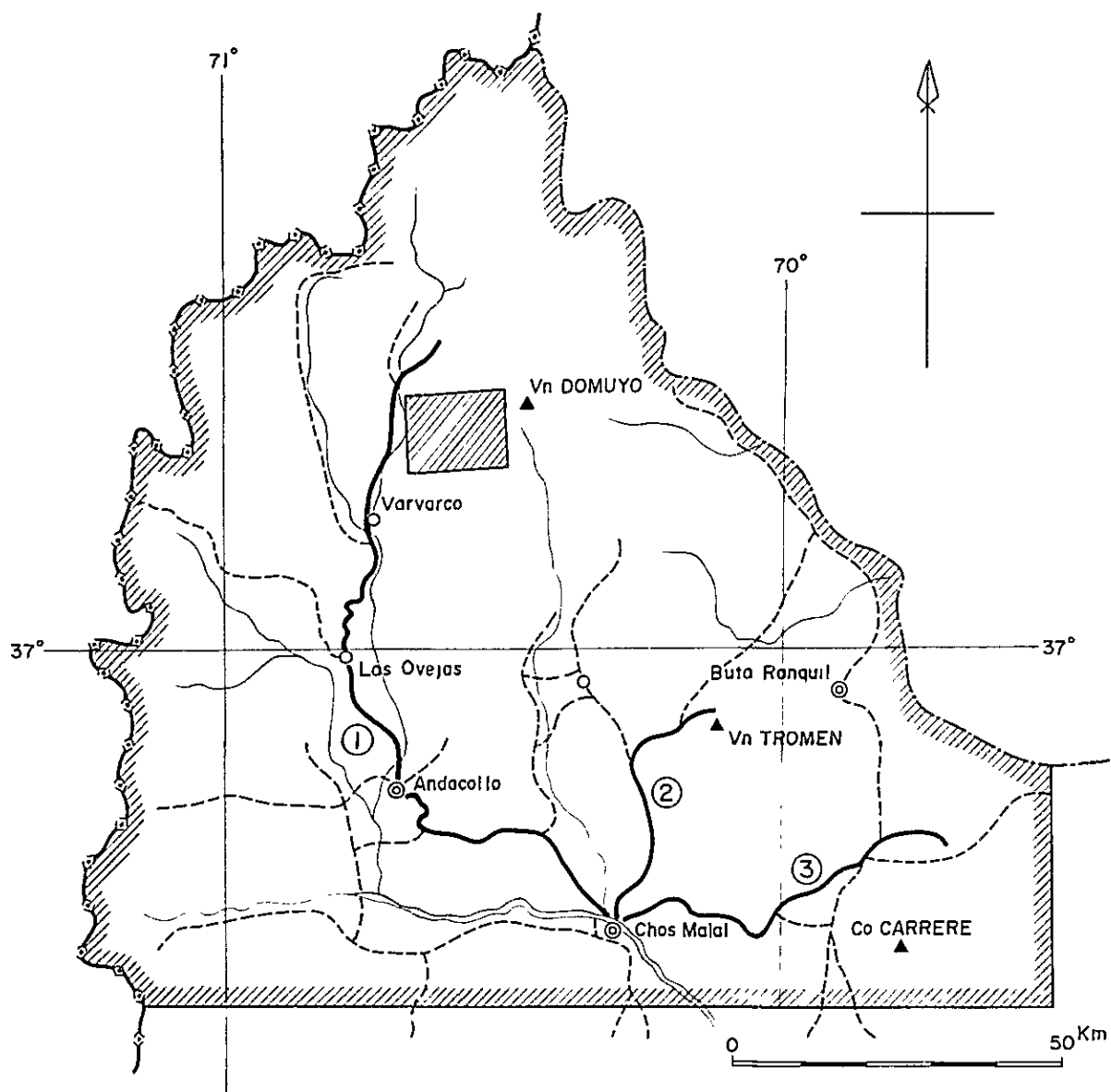


Fig.2-3 Geological interpretation map of aerial photographs



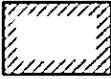
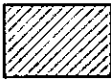

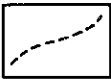
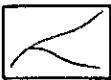
-  First phase survey area : 15,000 Km²
(Limite del area de 15,000 Km²)
-  Second phase survey area : 200 Km²
(Area seleccionada de 200 Km²)
-  Routes of reconnaissance geological survey
(Rutas de reconocimiento efectuadas)
-  Roads
(Rutas y accesos a la zona)
-  Rivers
(Detalle de drenaje)

Fig.2-4 Map of the survey areas and routes of reconnaissance geological survey

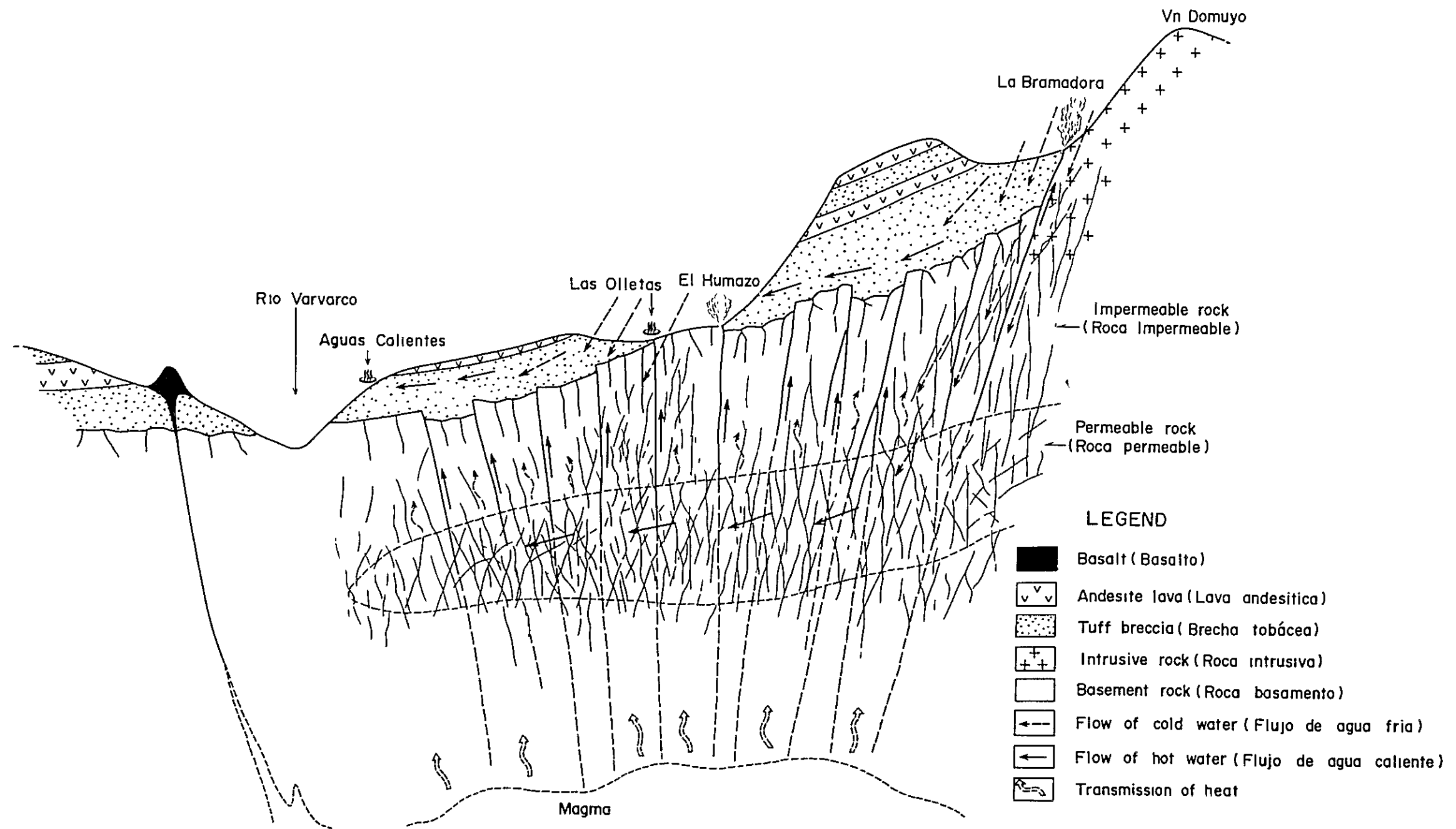


Fig.2-5 Schematic profile of geology and geothermal system

3. Geology in the Investigation Area

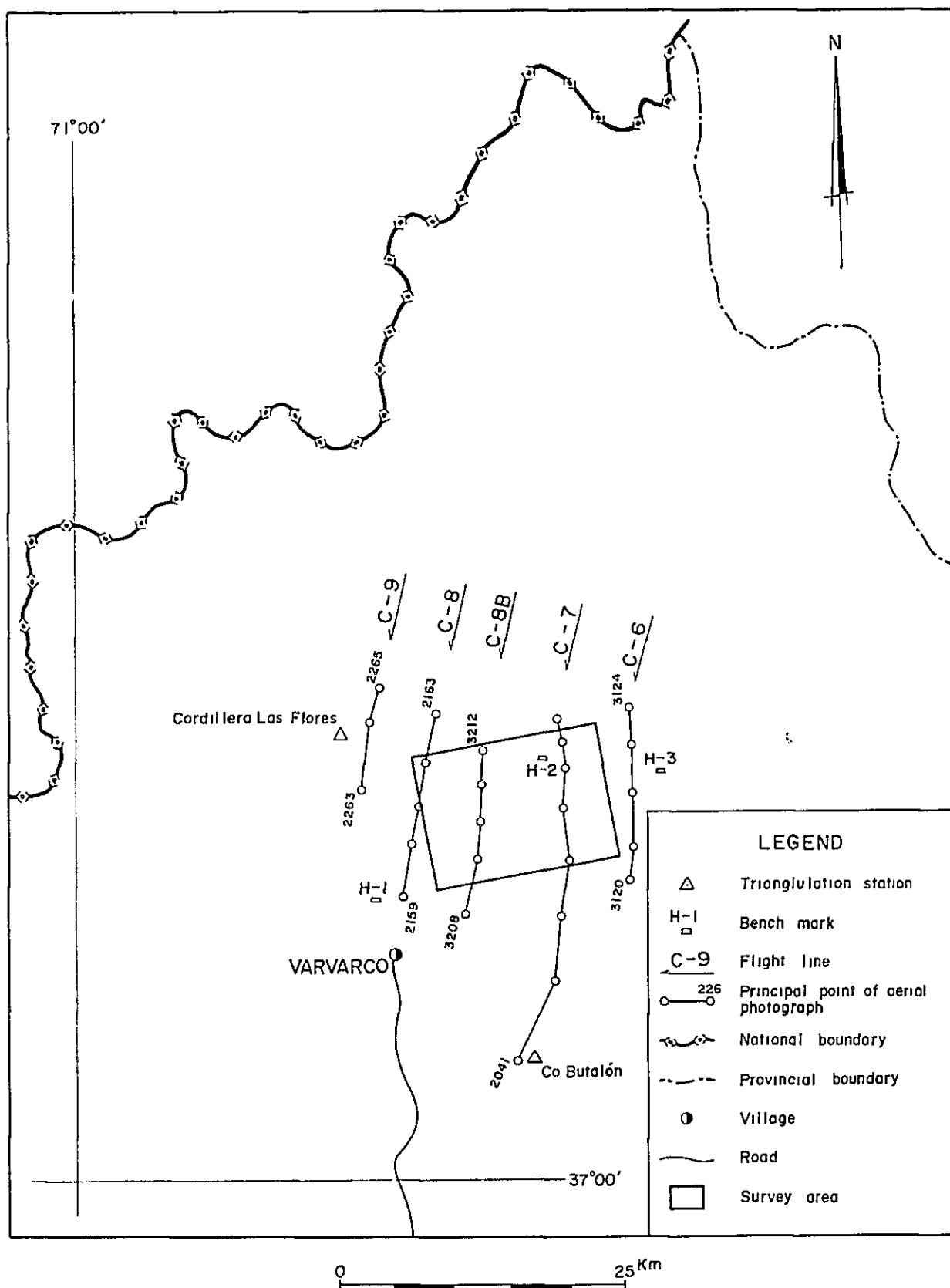


Fig.3-1 Principal points of aerial photographs and topographic standard points

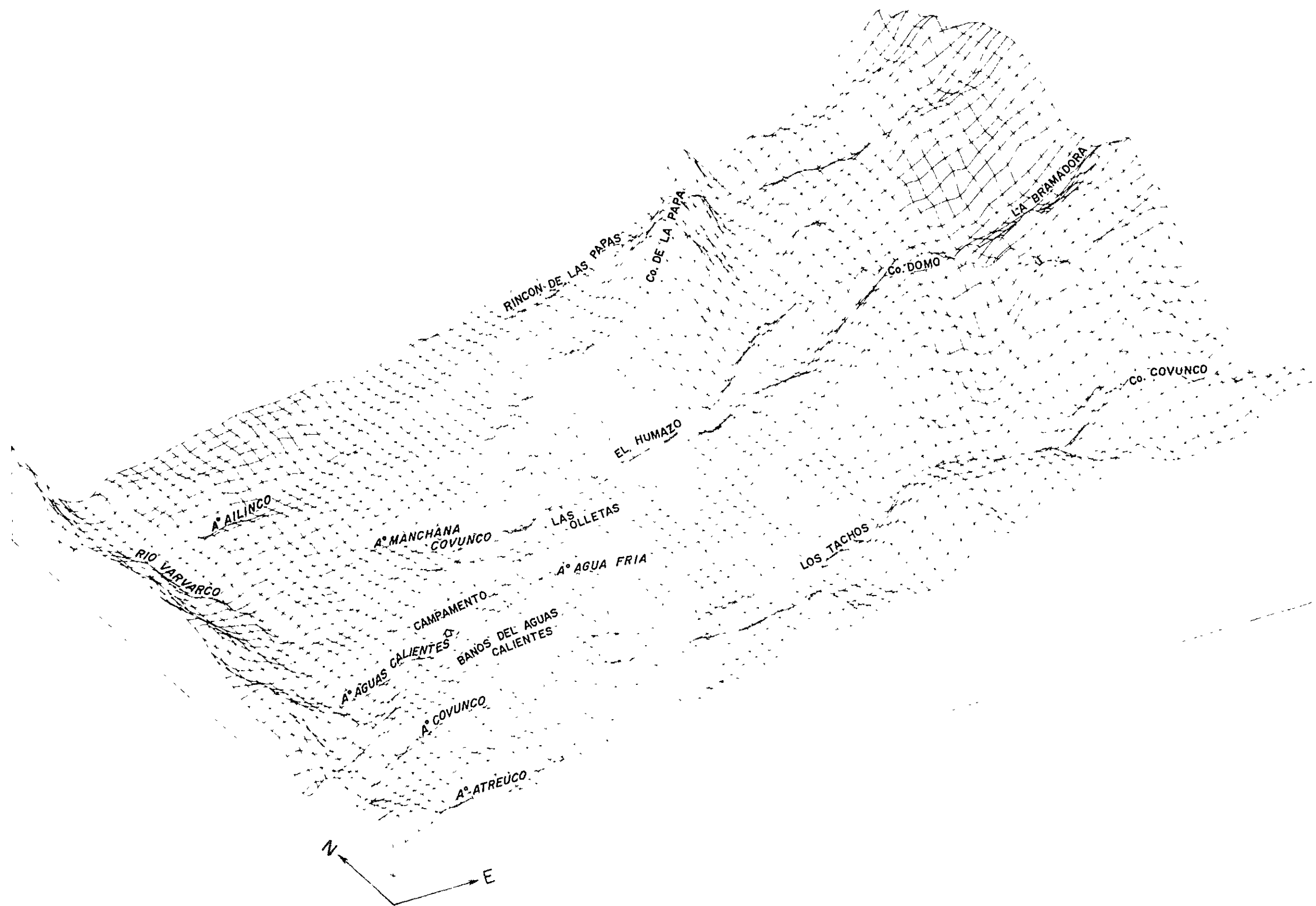


Fig.3-2 Bird's-eye view map of the survey area

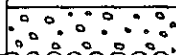
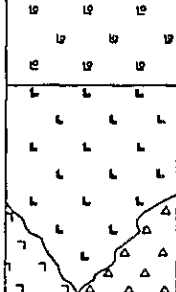


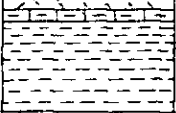

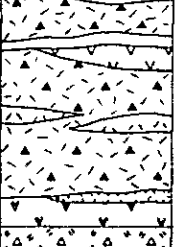

Age		Formation	Geological Column	Thickness	Lithology	Remarks
Quaternary	Holocene				Sand, Gravel (Terrace) Glacial deposits	
	Pleistocene	Volcanics of Co Domo		200 m 1200 m+	Rhyolite lava, Partially pumiceous Decite lava (including Perlitic layers) Dacitic tuff breccia	FT Age { 011±002 029±007 055±010 Distribution Southern half of the survey area
Tertiary - Quaternary		Acidic Pyroclastics F Sierra de Flores F Atreuco		200 m 1000 m	Pumiceous tuff Andesitic volcanic breccia Andesite (dike) Welded tuff Andesitic tuff breccia (Scoria tuff) Andesite lava	FT Age 011±003 Distribution Northern half of the survey area
Tertiary	Pliocene - Miocene	andesite		100 m 500 m	Andesite lava Granodiorite - porphy (intrusive) Andesitic tuff breccia	Locality Co Domo and Los Tachos
Jurassic	Malm - Dogger	F Tordillo		100 m 450 m	Dacitic tuff, Sandy tuff (thin deds) Limestone, Calcareous siltstone Red ~ green sandstone, shale	Locality La Bramadora
		F Auquico		100 m 500 m	White mudstone, green sandstone Limestone Gypsum beds	Locality La Bramadora
		F Chacoy Melahue		550 m 1000m+	Black mudstone Andesitic tuff breccia Black mudstone Andesite lava Andesitic lapilli tuff Red sandstone (thickness 1~2cm) Basalt lava Basaltic lapilli tuff ~ andesitic tuff	Locality El Humazo La Bramadora Rincón de Las Papas
		Basement			Peilitic hornfels, Psammitic hornfels Basic hornfels (Partially sandy) Peilitic schist, Psammitic schist Granite, aplite Granodiorite (including xenoliths of silicified rock) Basalt (dyke)	K-Ar Age { 227±16 259±13 Locality El Humazo Rincón de Las Papas Locality Rio Varvarco A° Atreuco, A° Covunco A° Manchona Covunco

Fig.3-3 Geological columnar section of the survey area

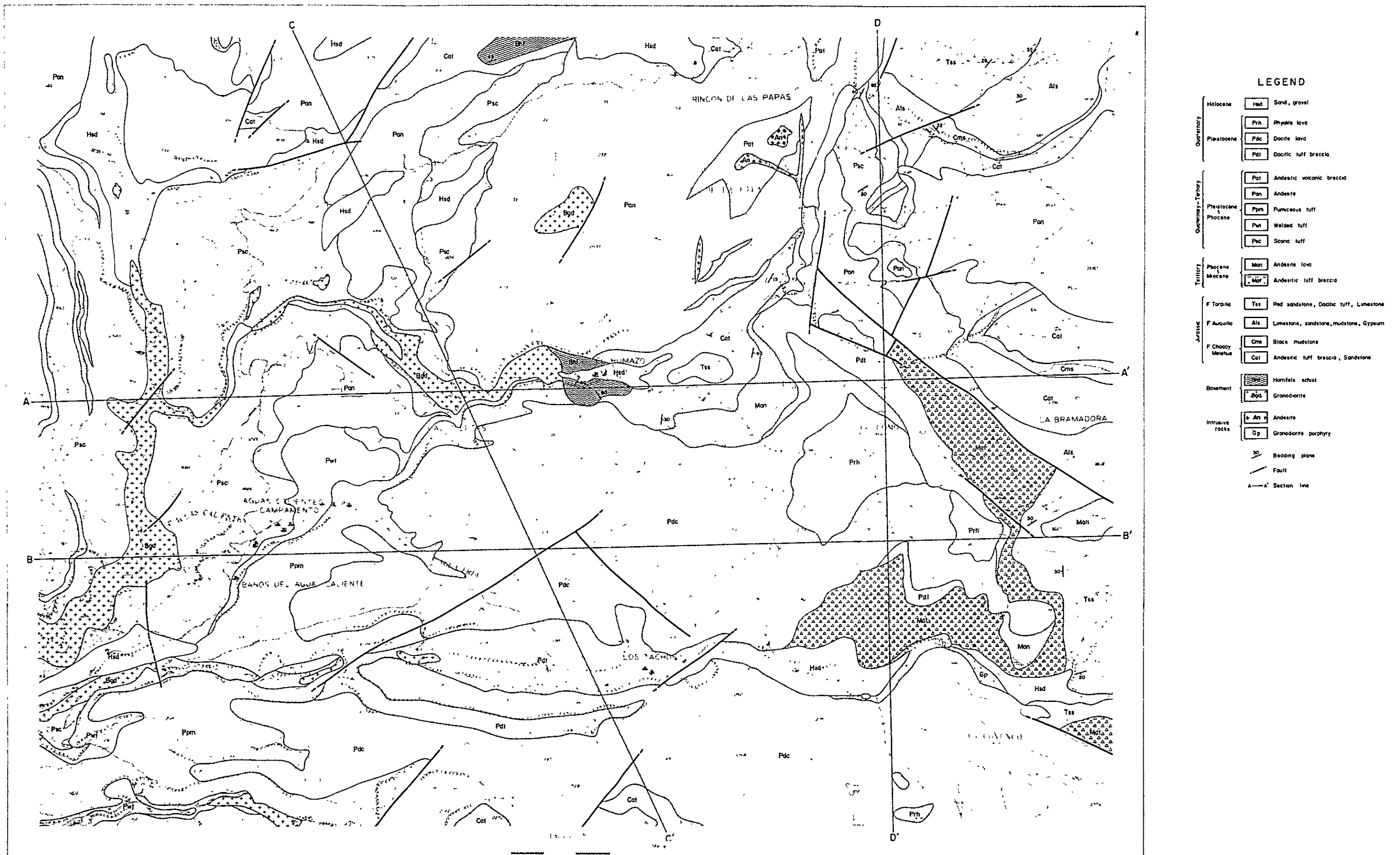


Fig.3-4 Geological map of the survey area

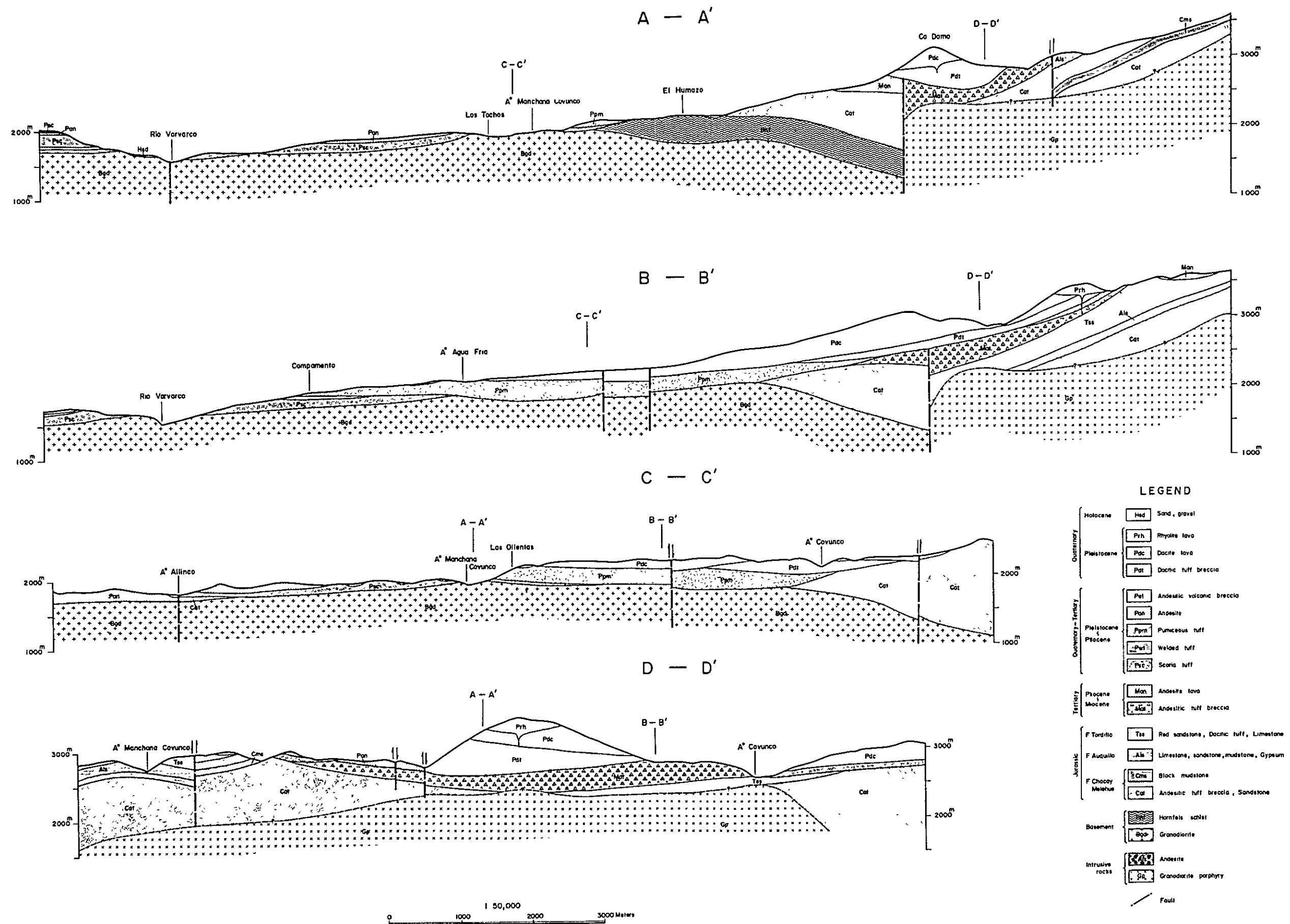
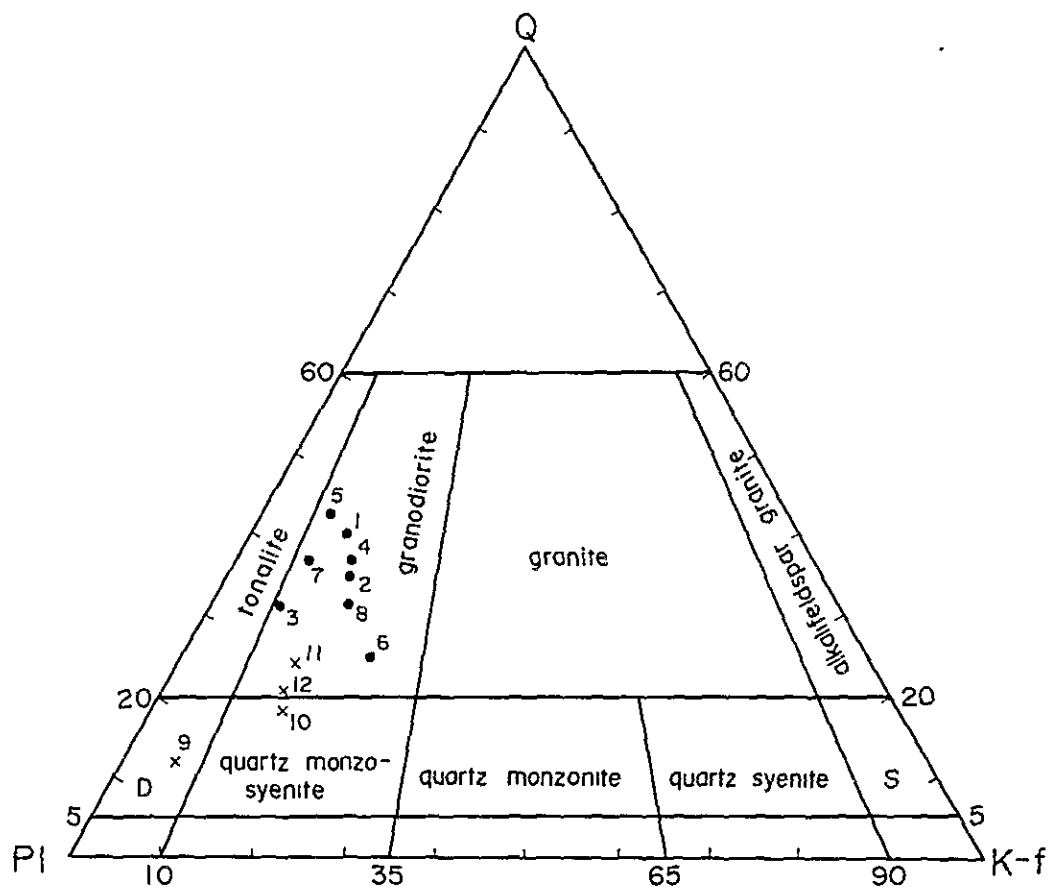


Fig.3-5 Geological cross-sections



Varvarco intrusive	{	1 : F-1	5 : TM-11
		2 : F-26	6 : TM-16
		3 : F-42-2	7 : TM-27
		4 : TM-8	8 : 83-2-12-5
Domuyo complex	{	9 : F-14	10 : TM-12
		11 : TM-48	12 : TM-201

D : quartz diorite etc

S : alkali feldspar-quartz syenite

Fig.3-6 Modal diagram of quartz - potash feldspar plagioclase

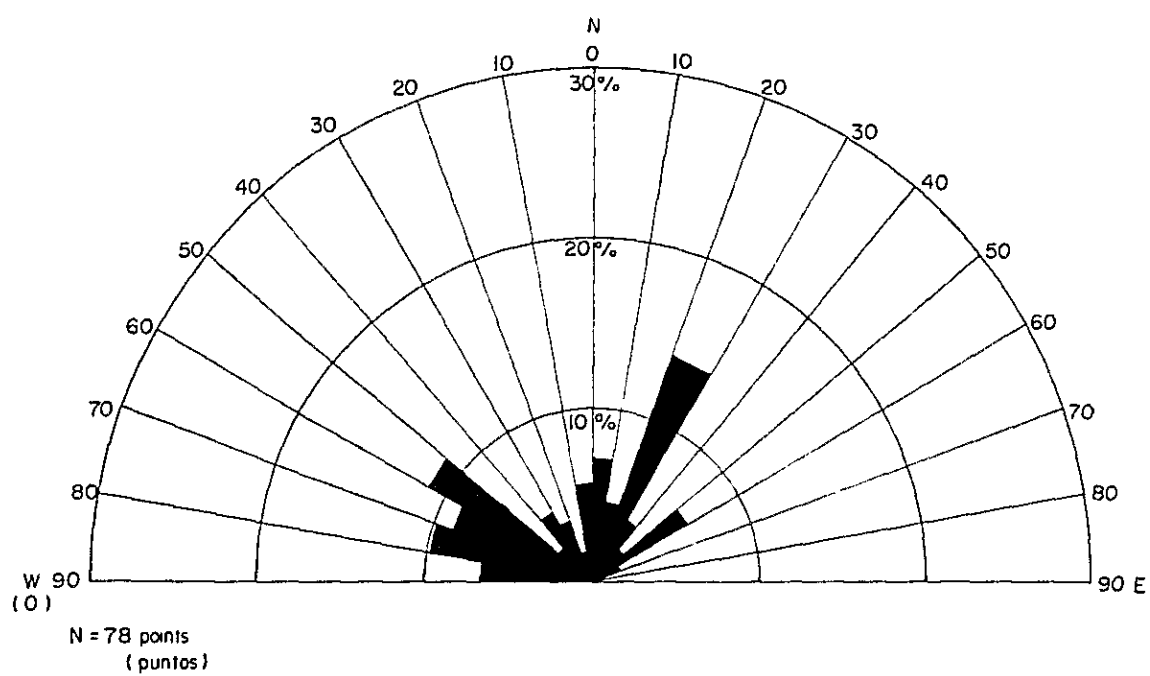


Fig.3-7 Rose diagram of joints in granodiorite

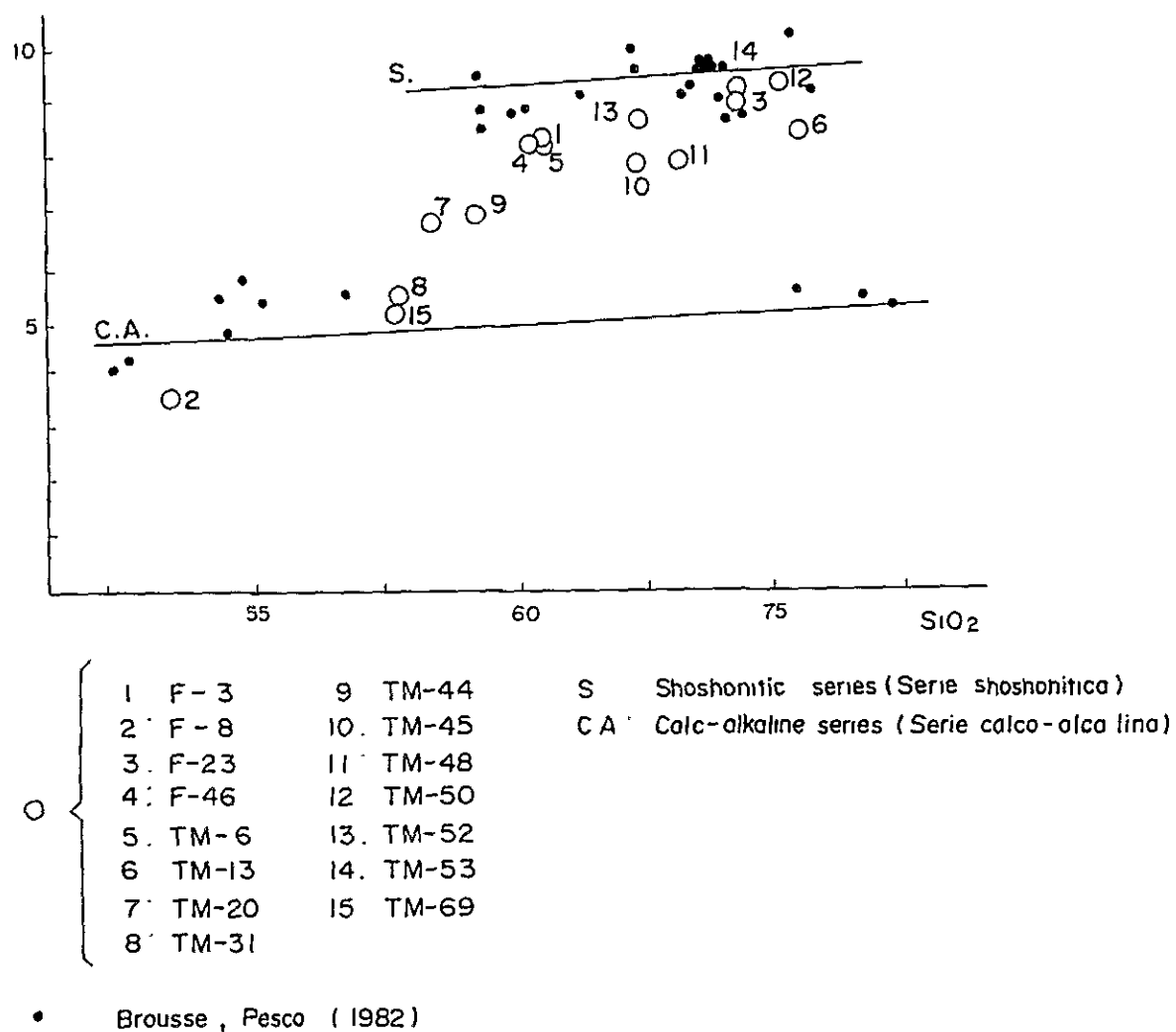
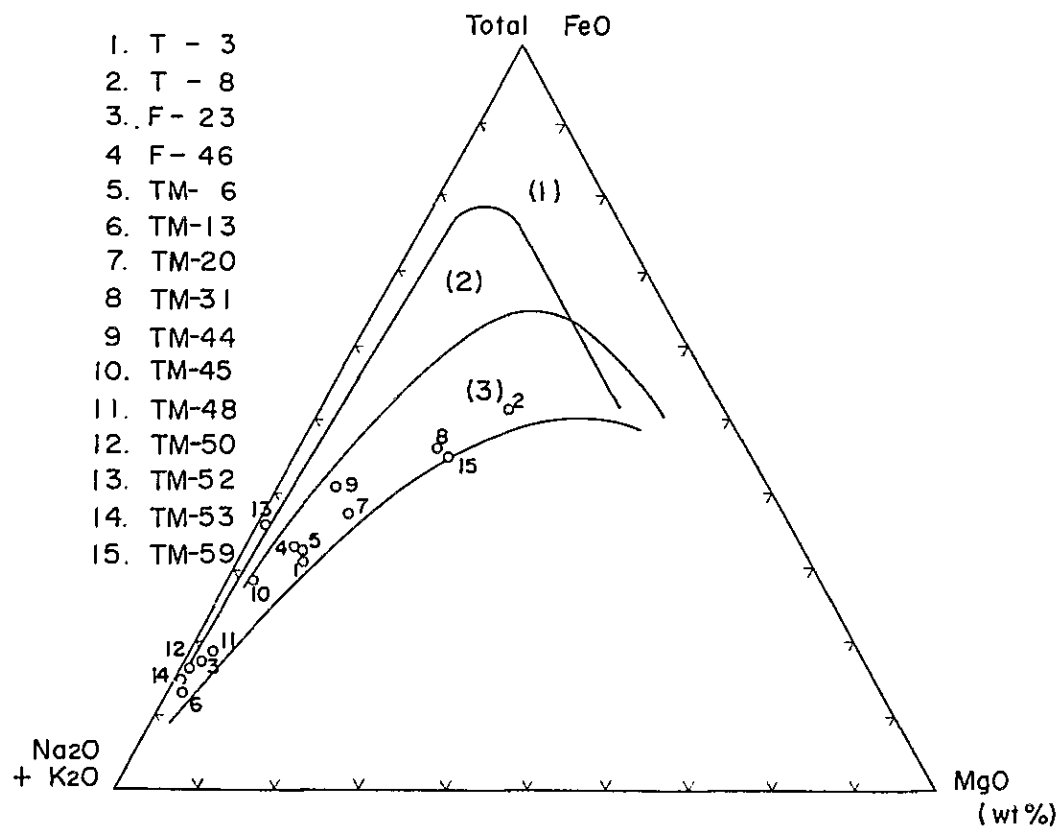
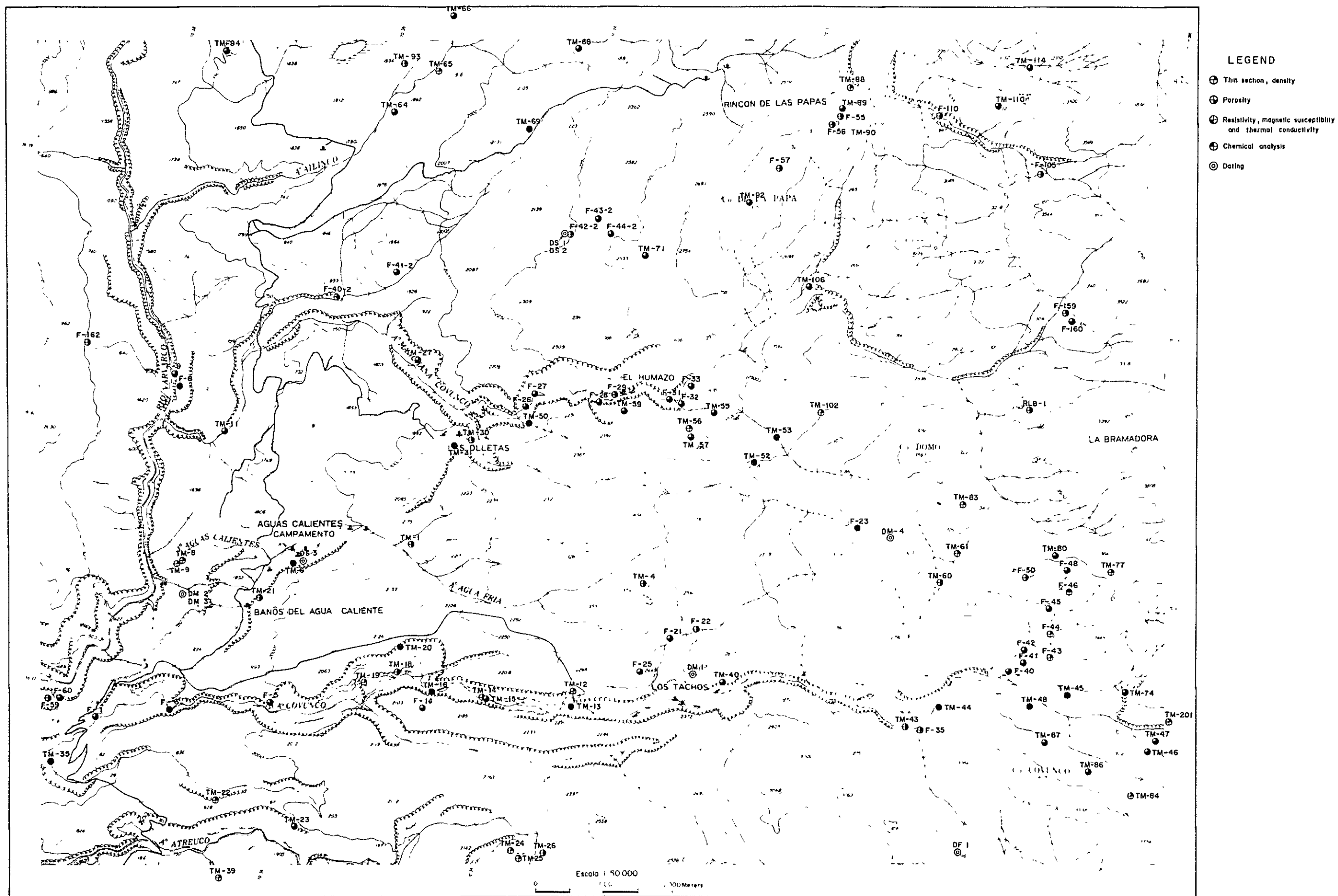


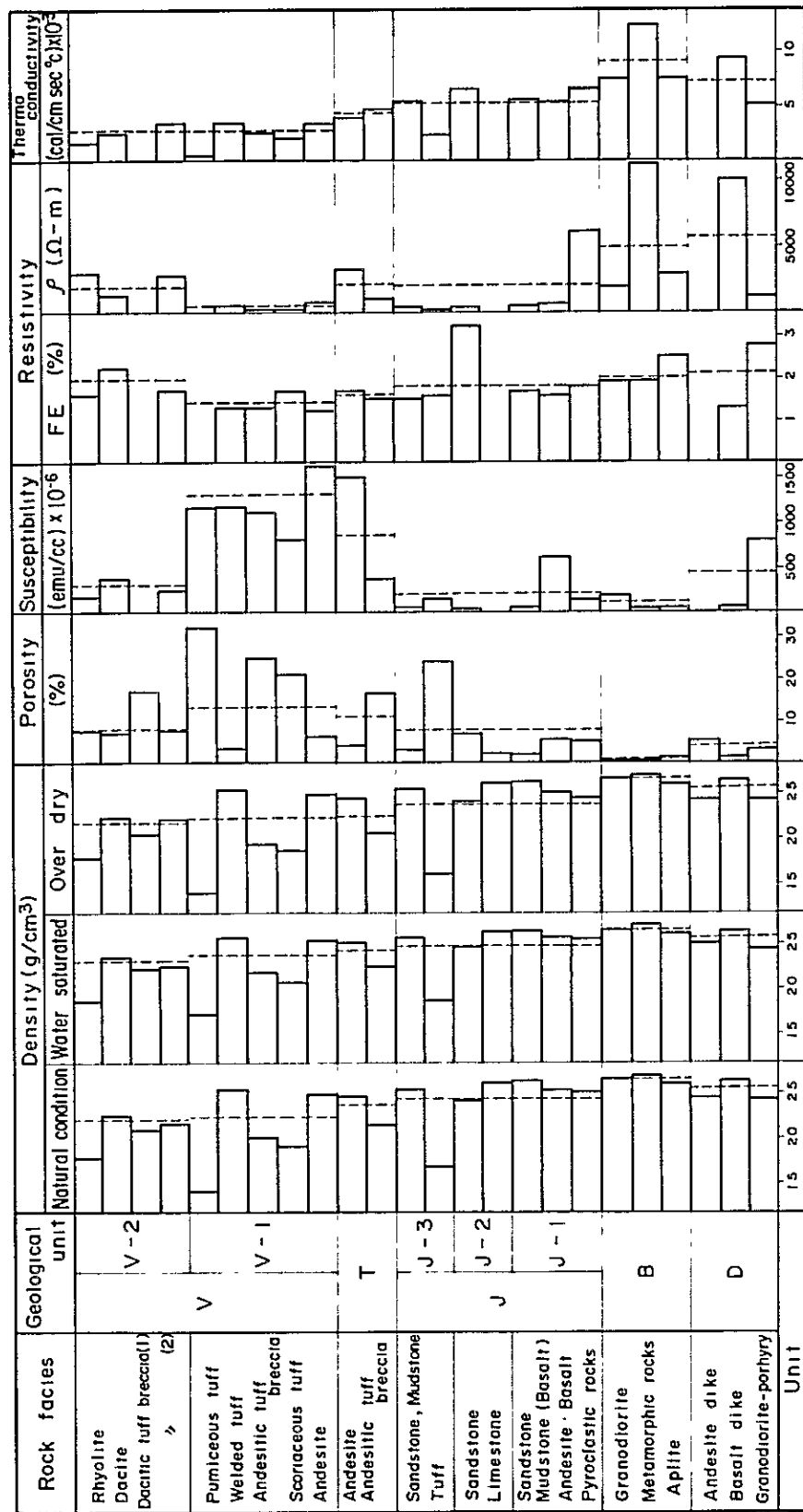
Fig.3-8 Alkali - silica diagram of younger volcanic rocks



- (1) Chemical variation in rocks of Skaergaard intrusion
- (2) Chemical variation in tholeiitic volcanics of Izu-Hakone area, Japan
- (3) Chemical variation in calc-alkaline volcanics of Izu-Hakone area, Japan

Fig.3-9 MgO - total FeO - (Na₂O + K₂O) diagram of younger volcanic rocks





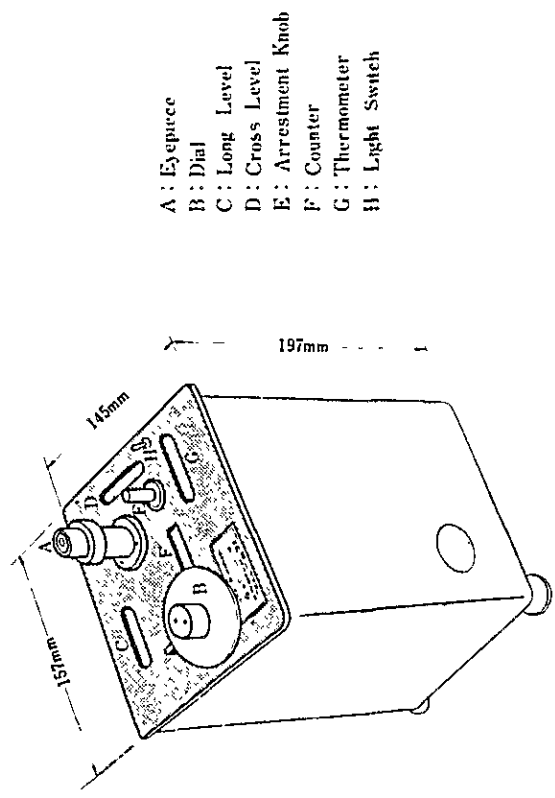
Mean value of rock facies, ----- Mean value of geological unit

V Quaternary - Tertiary
V-2 Pleistocene, Volcanics of Co Domo
V-1 Pleistocene - Pliocene, Tertiary, Pliocene - Miocene, Andesite
Acidic Pyroclastics J-3 Tordillo Formation
Sierra de Flores Formation J-2 Auquico Formation
Aireuco Formation J-1 Chacay Melehue Formation
B Basement
D Dike rock etc

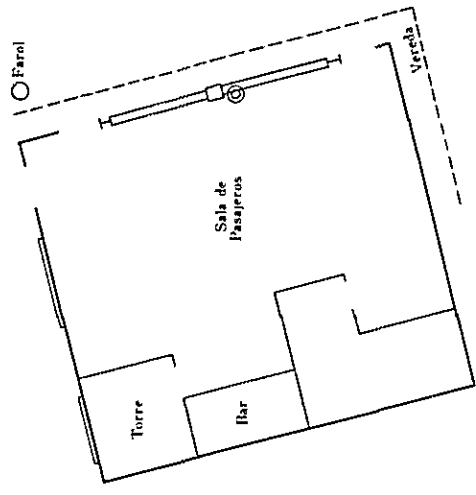
Fig.3-11 Physical properties of rocks

4. Geologic Structure in the Investigation Area

•



- A : Eyepiece
- B : Dial
- C : Long Level
- D : Cross Level
- E : Arrestment Knob
- F : Counter
- G : Thermometer
- H : Light Switch



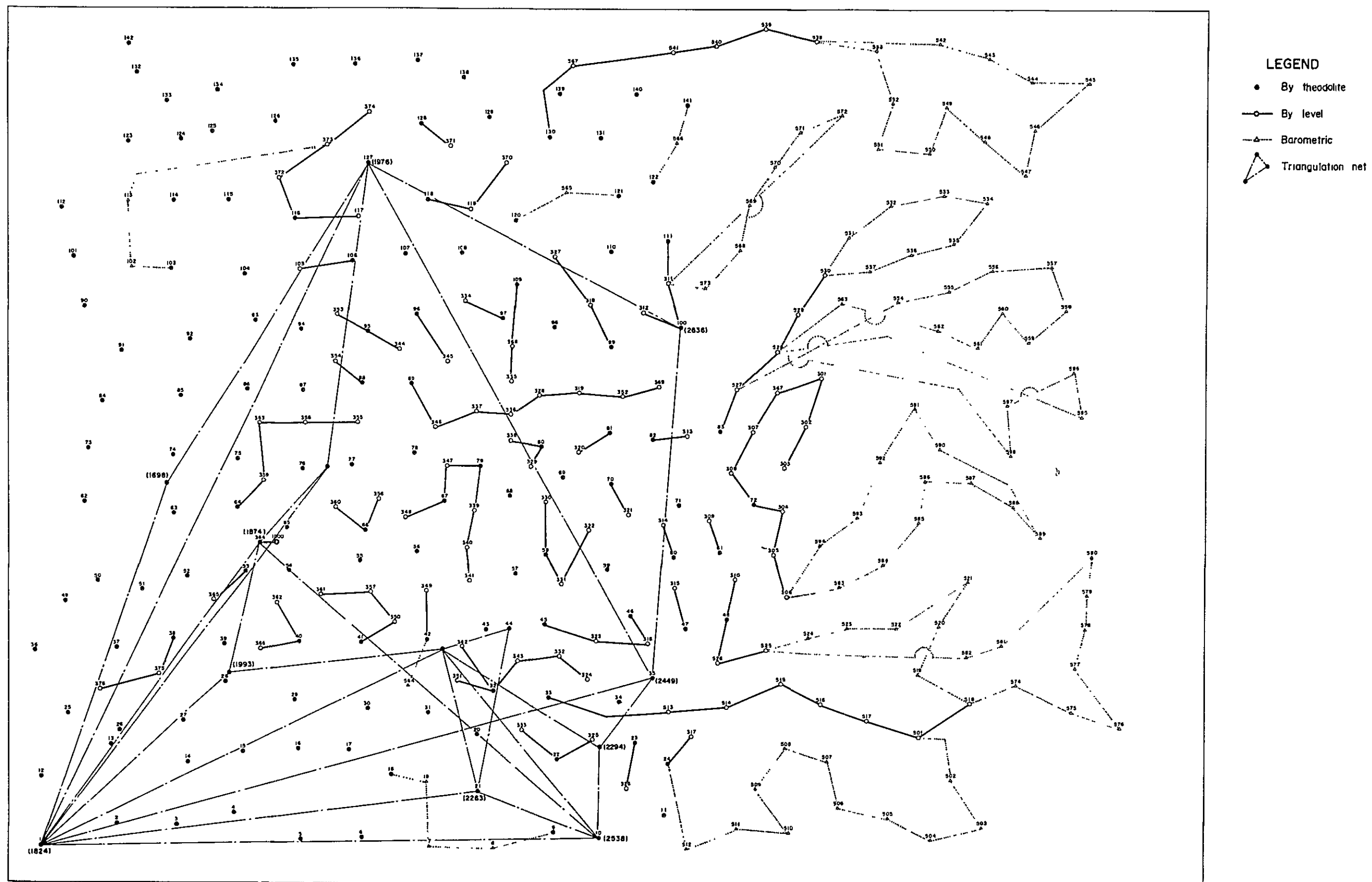


Fig.4-3 Network of leveling

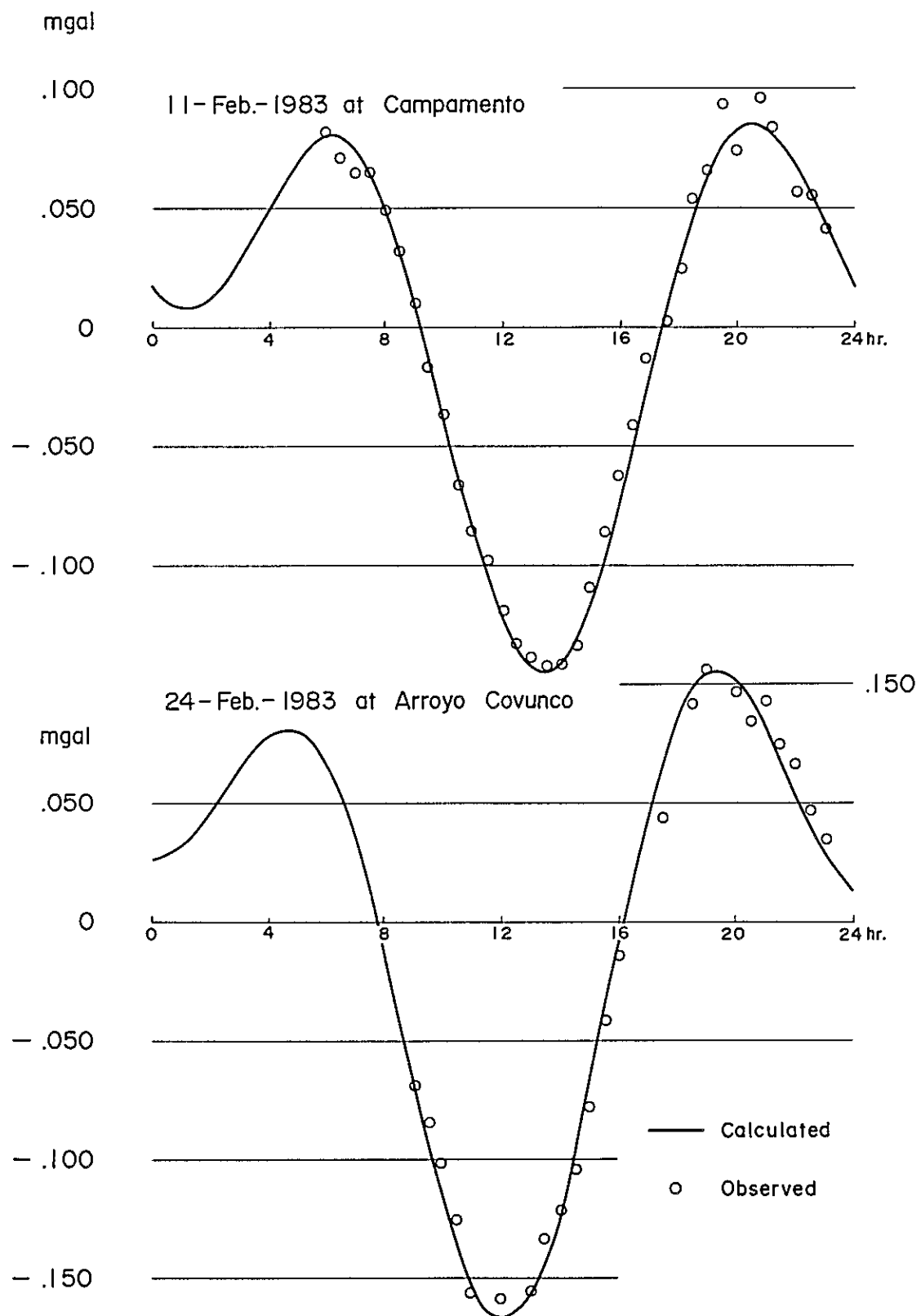


Fig.4-4 Observations of diurnal gravity variation

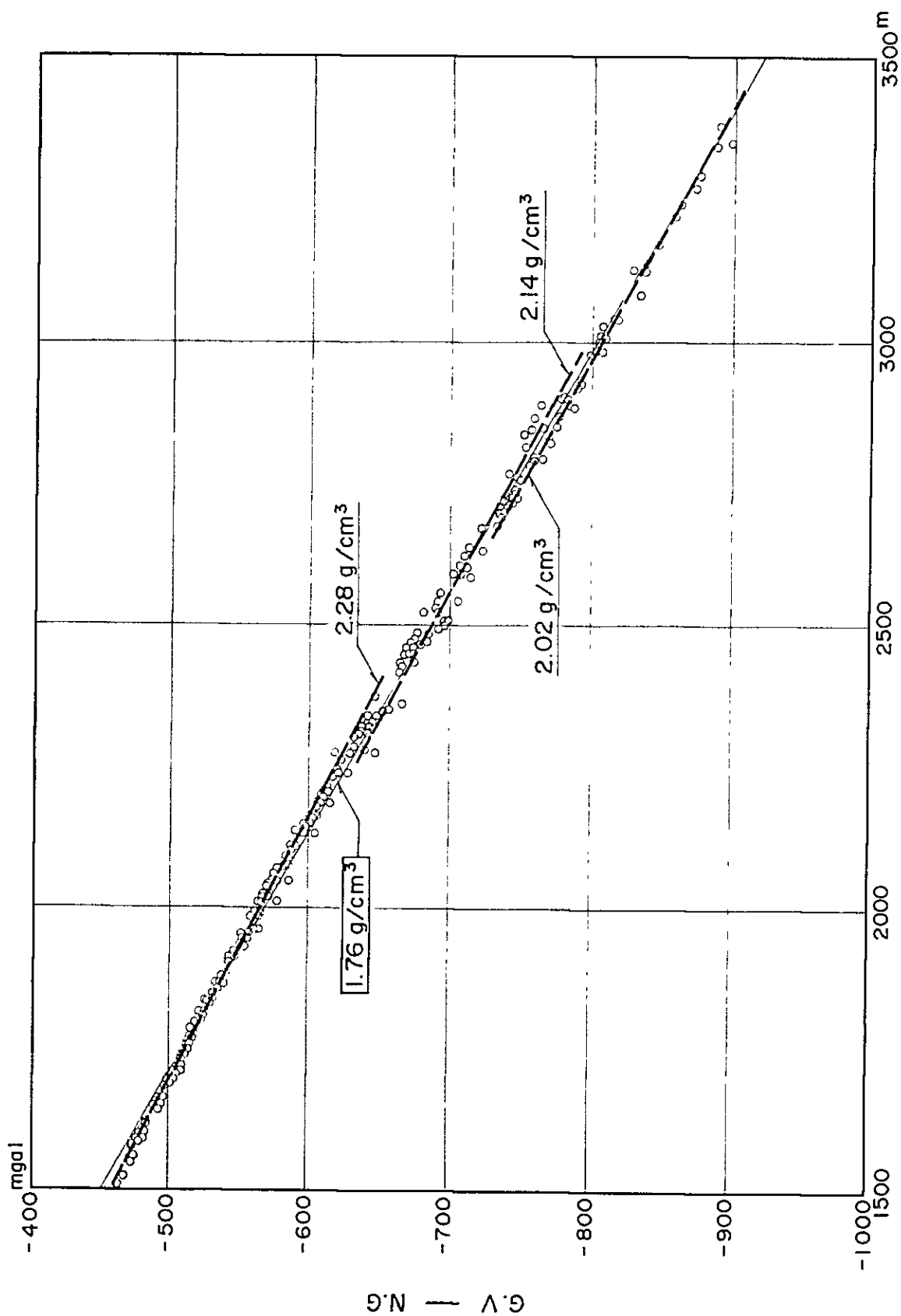


Fig.4-5 Relation between gravity and altitude

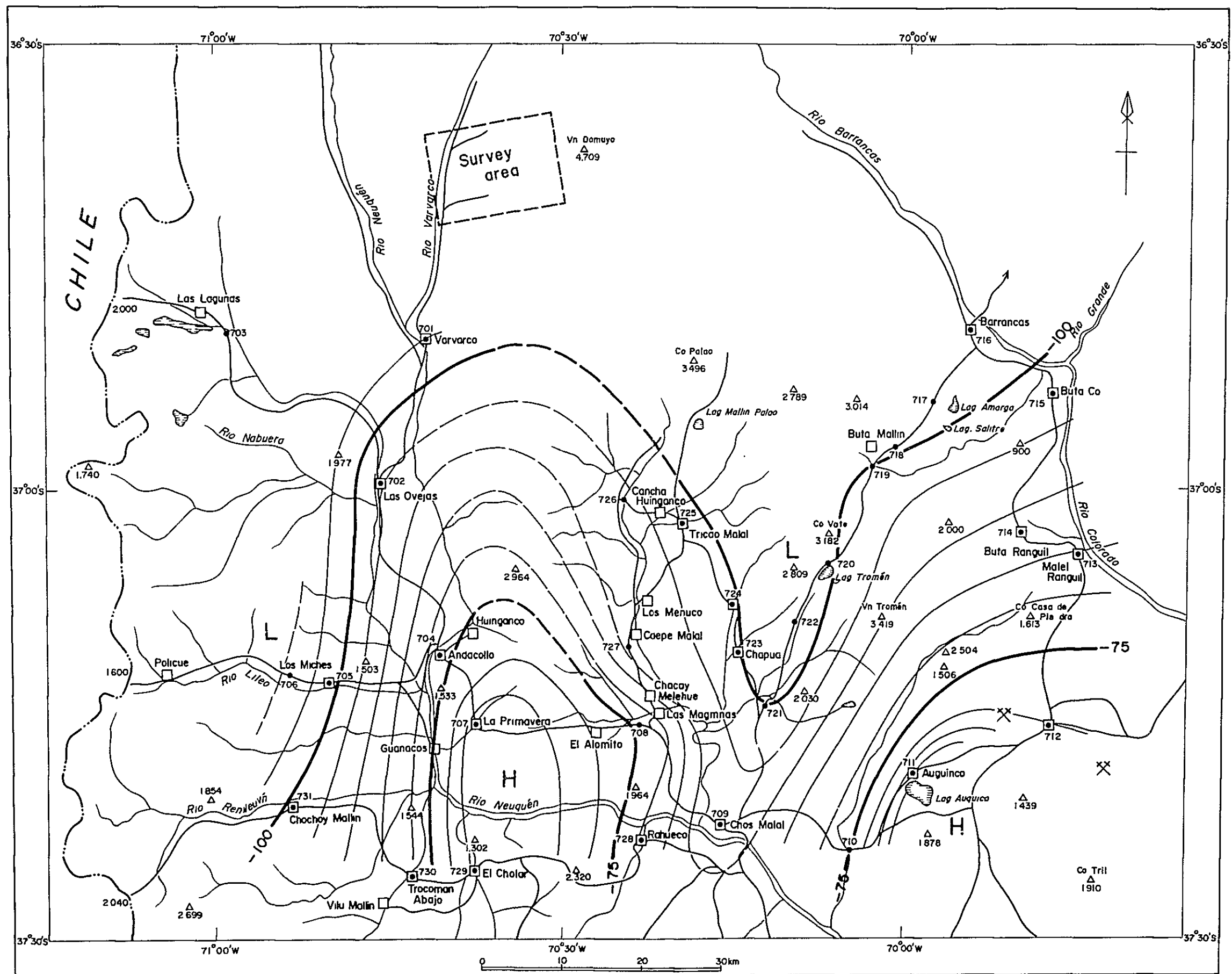


Fig.4-6 Regional Bouguer anomaly map ($\rho = 2.30 \text{ g/cm}^3$)

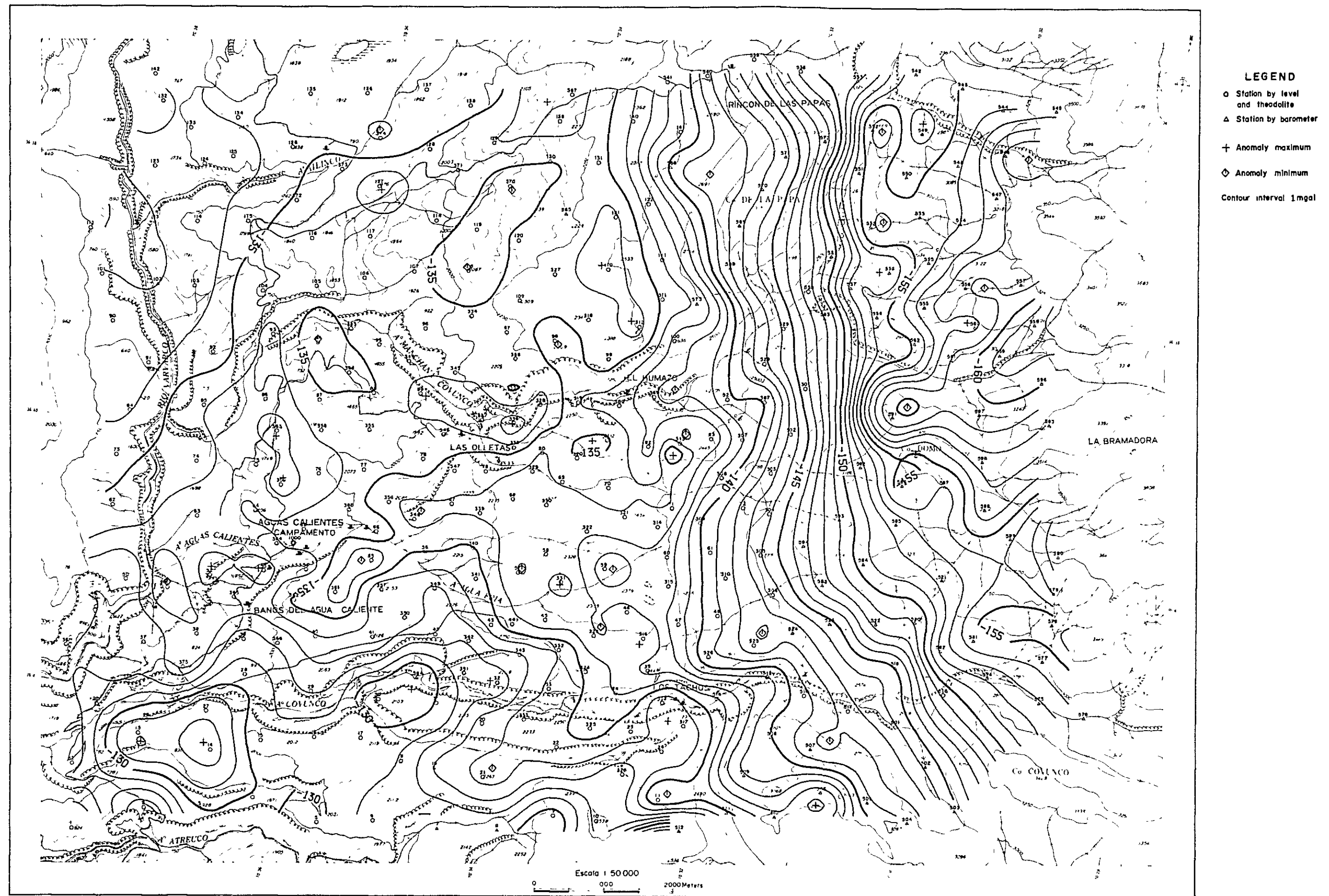


Fig.4-7 Bouguer anomaly map ($\rho = 2.30 \text{ g/cm}^3$)

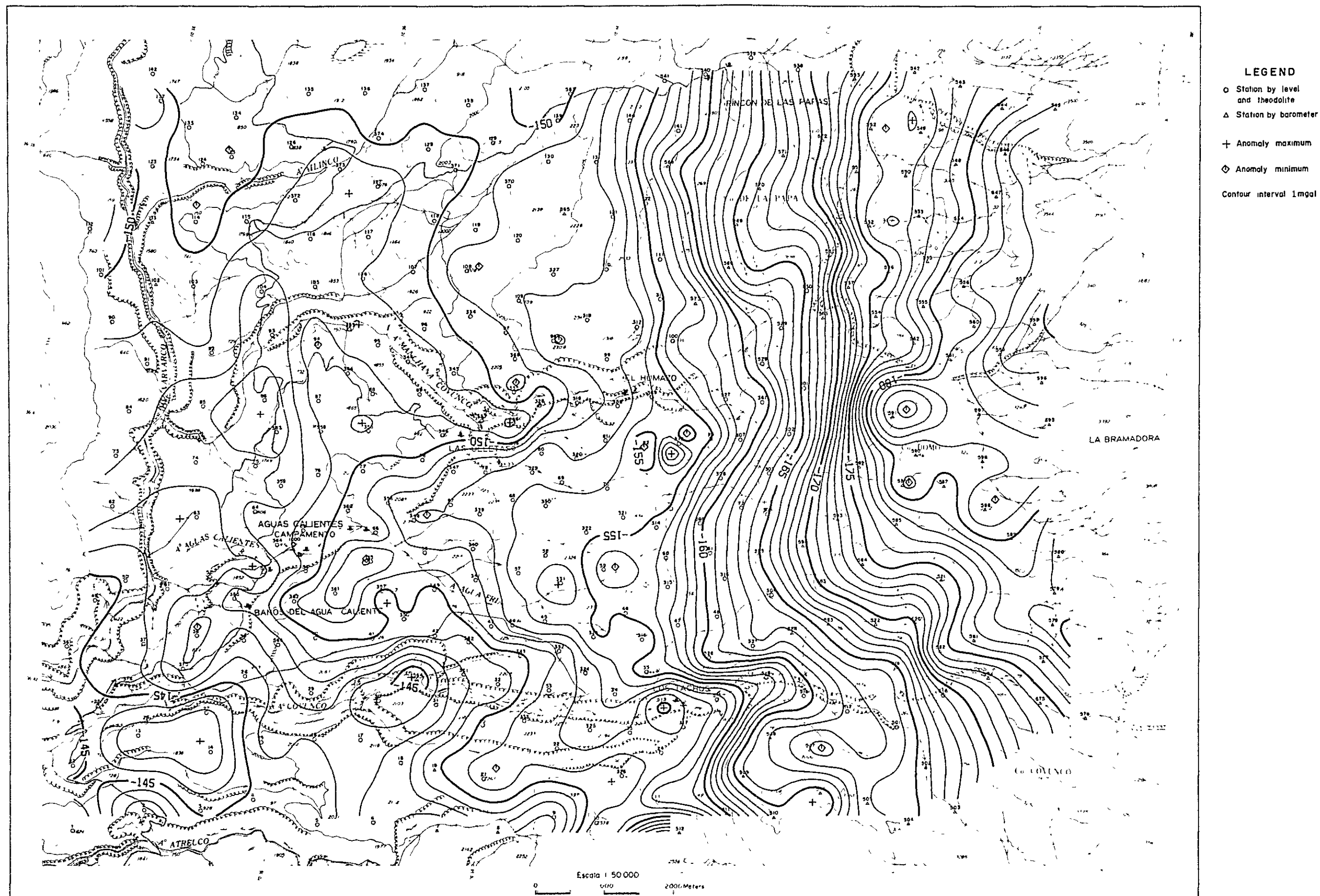


Fig.4-8 Bouguer anomaly map ($\rho = 2.00 \text{ g/cm}^3$)

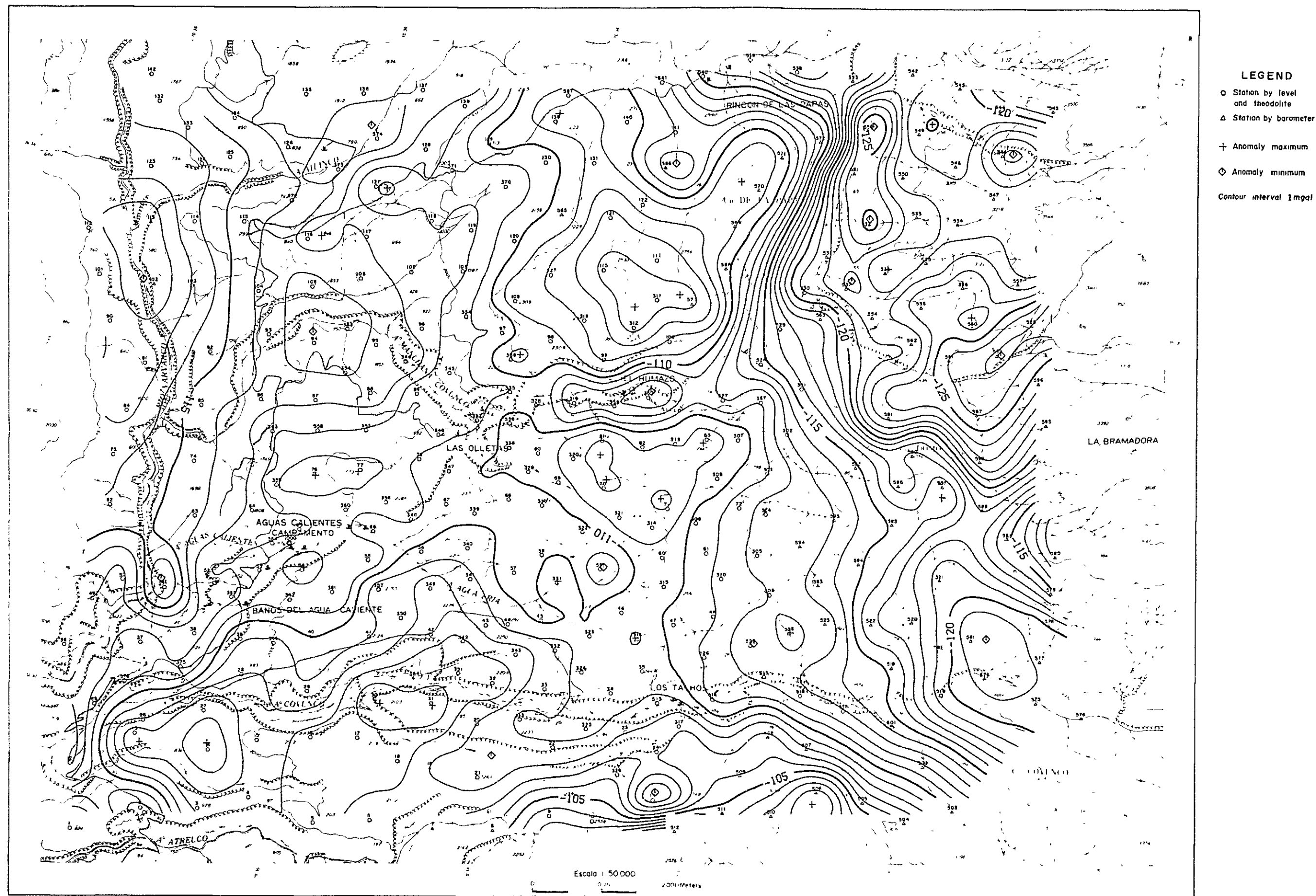


Fig.4-9 Bouguer anomaly map ($\rho = 2.50 \text{ g/cm}^3$)

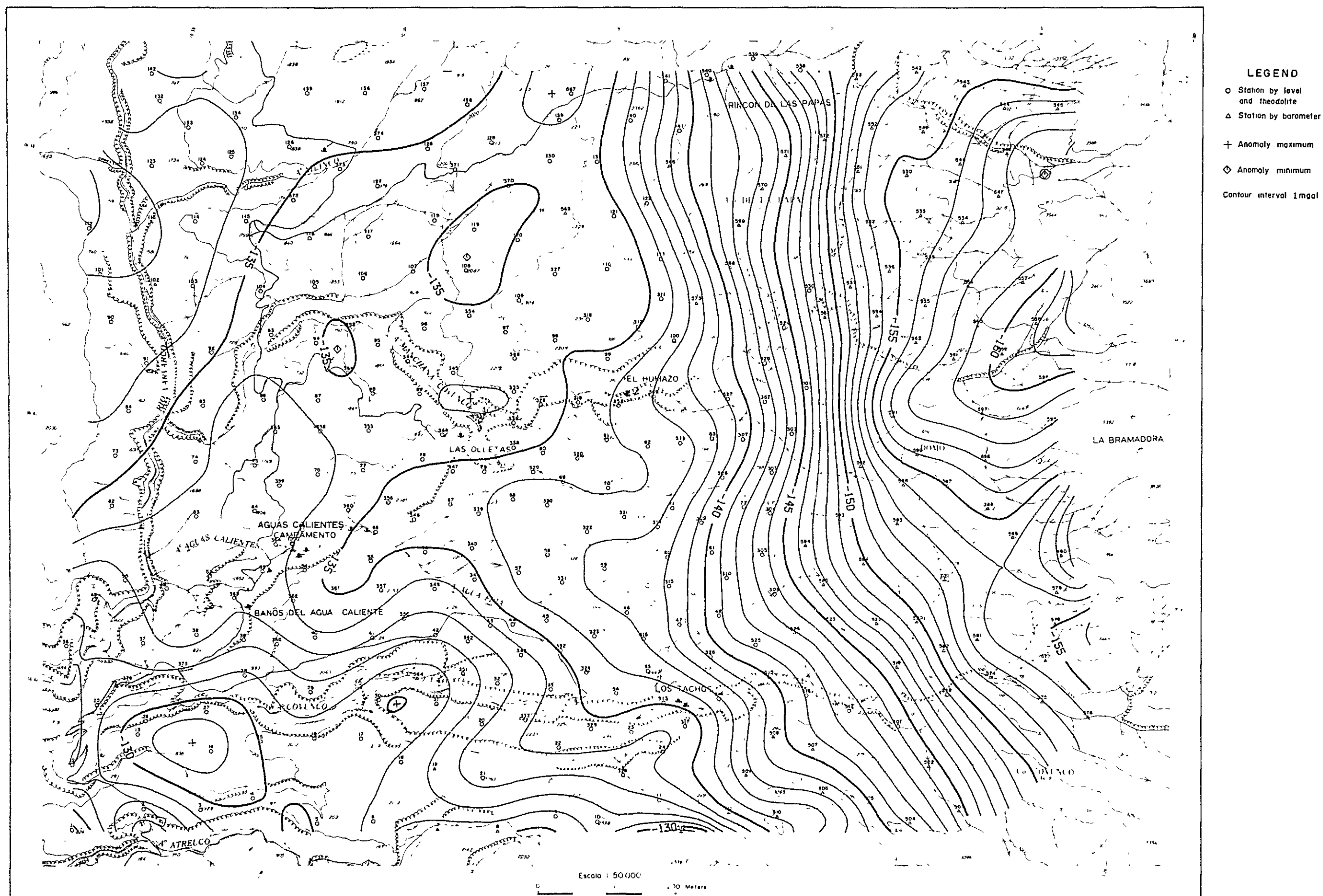


Fig.4-10 Long-wave Bouguer anomaly map ($\rho = 2.30 \text{ g/cm}^3$)

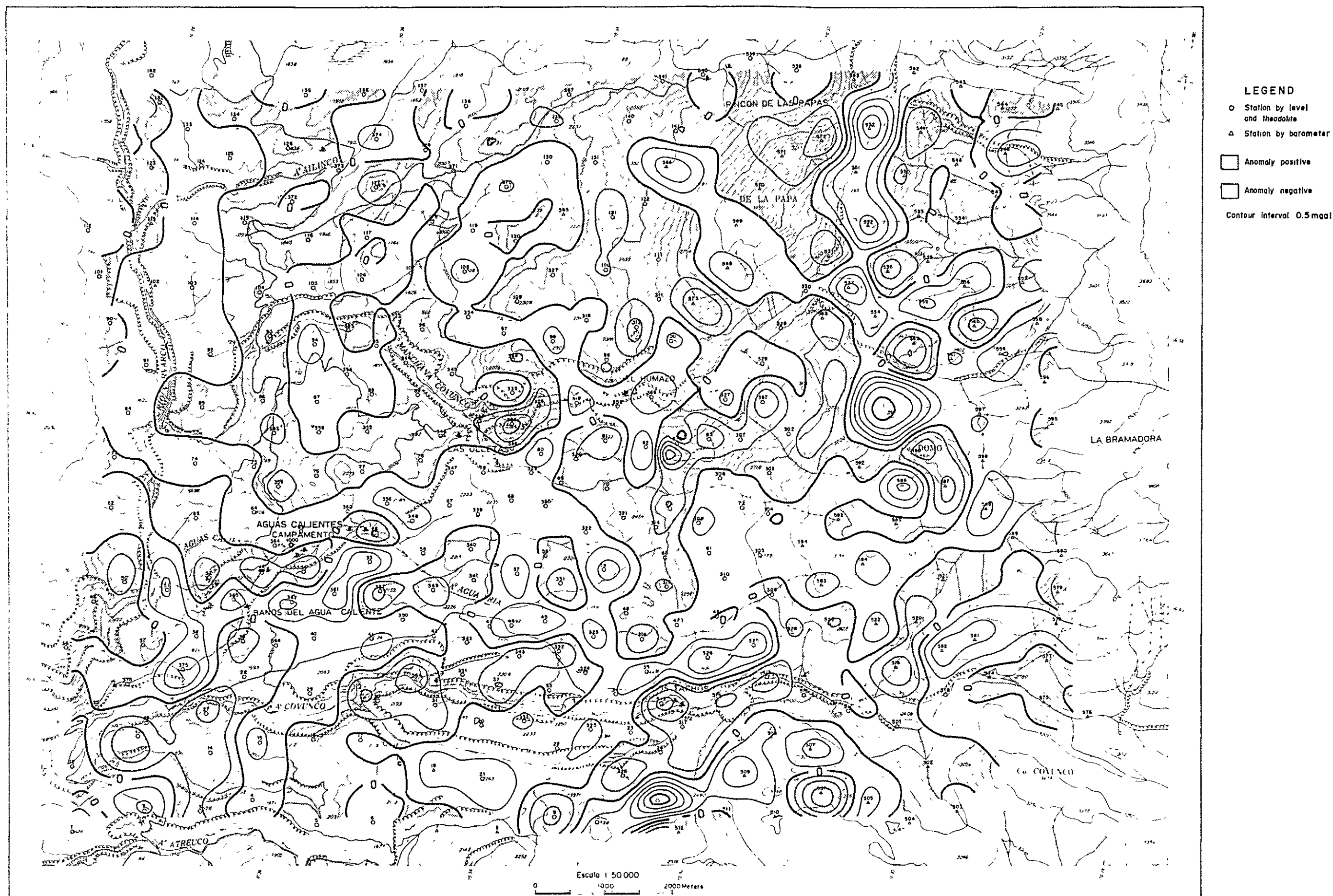
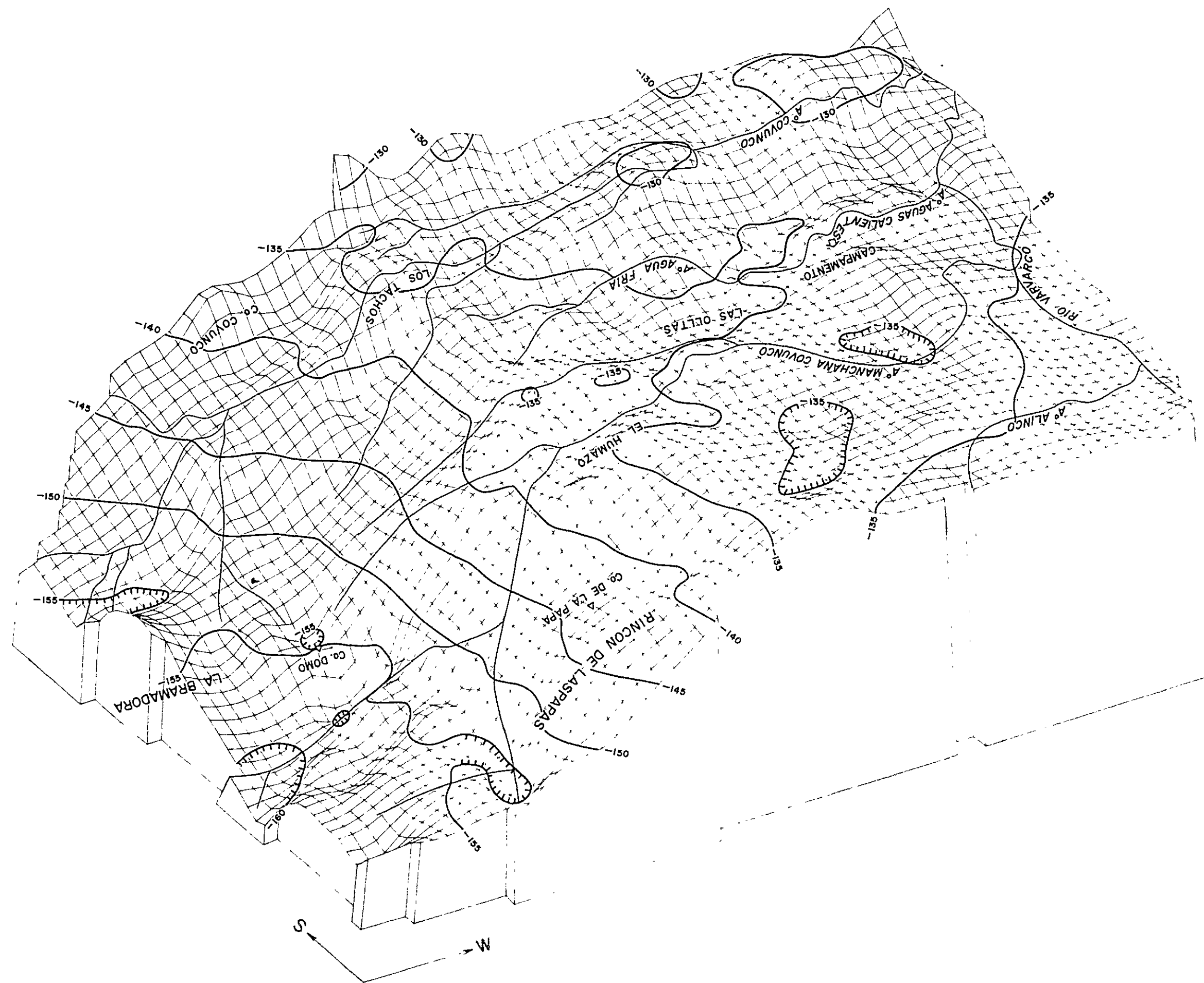


Fig.4-11 Short-wave Bouguer anomaly map ($\rho = 2.30 \text{ g/cm}^3$)



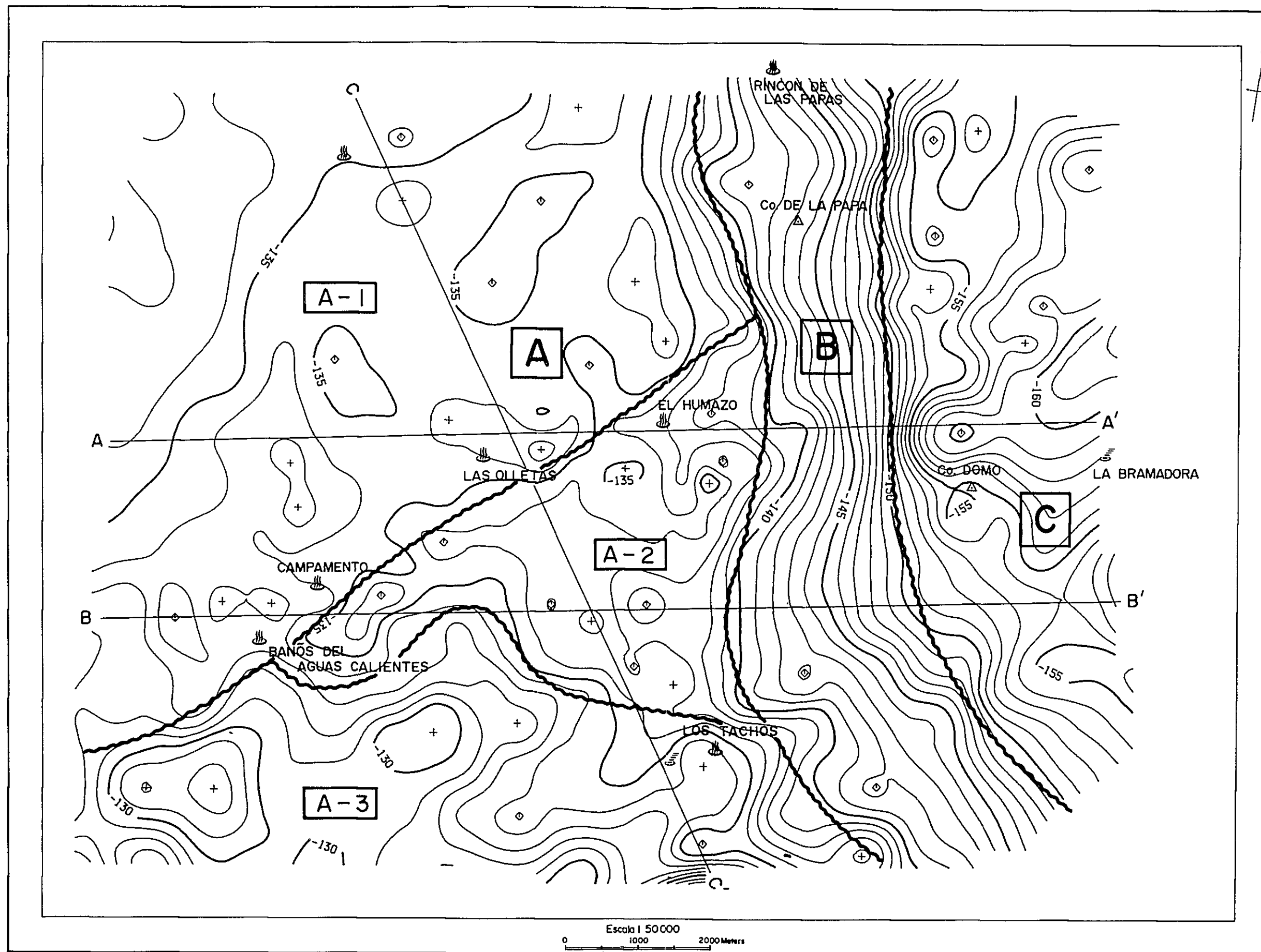


Fig.4-13 Zoning of Bouguer anomaly map

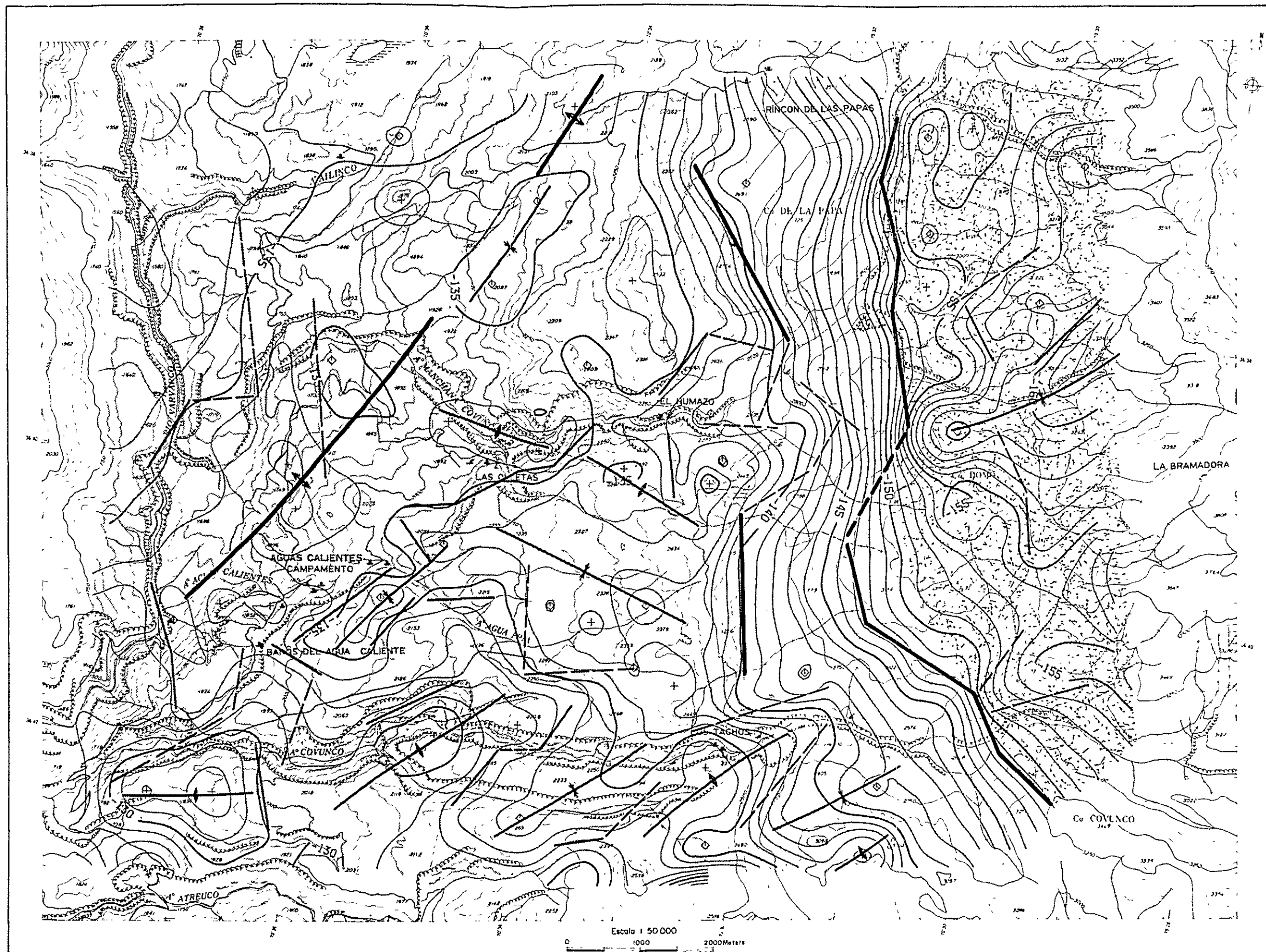


Fig.4-14 Gravimetric interpretation map

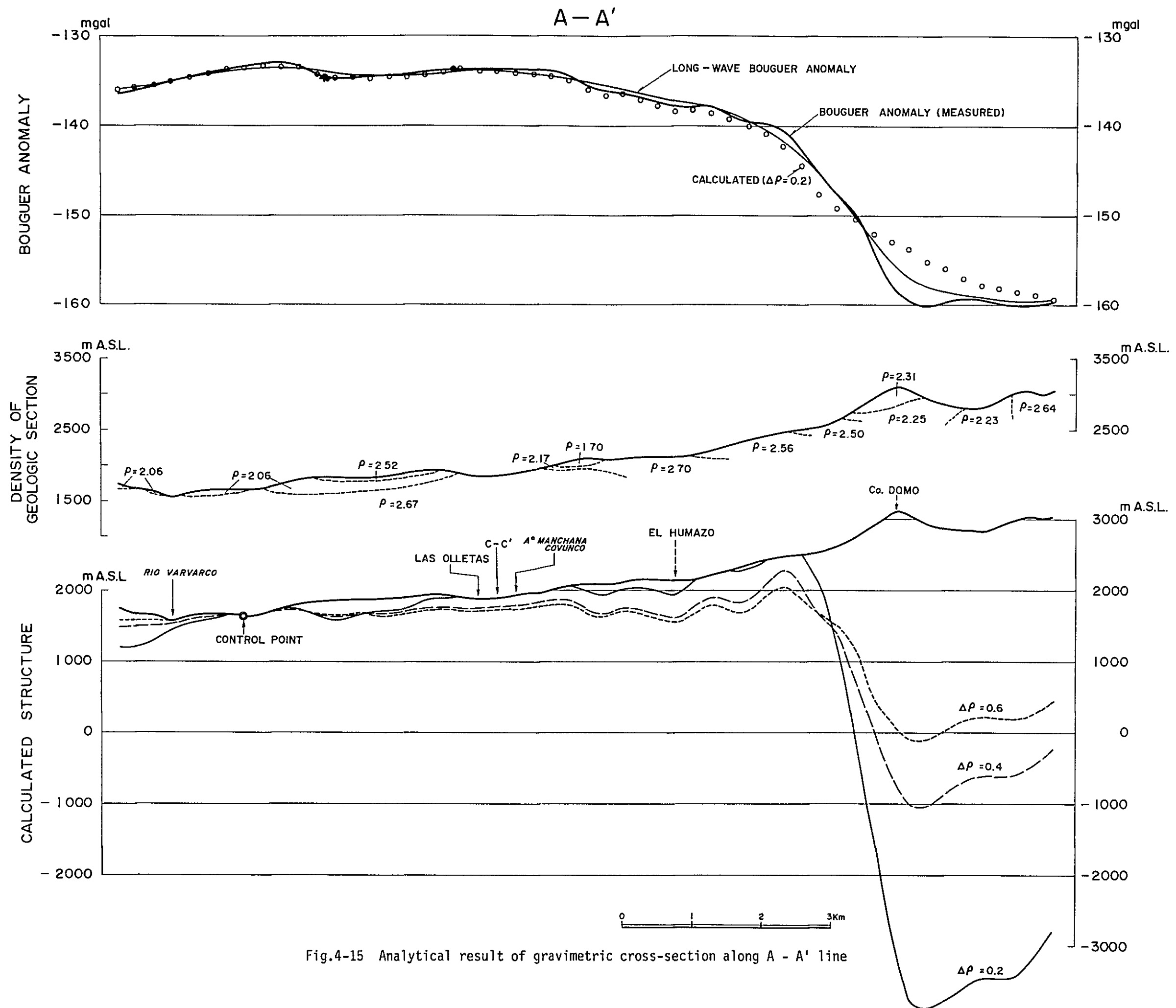


Fig.4-15 Analytical result of gravimetric cross-section along A - A' line

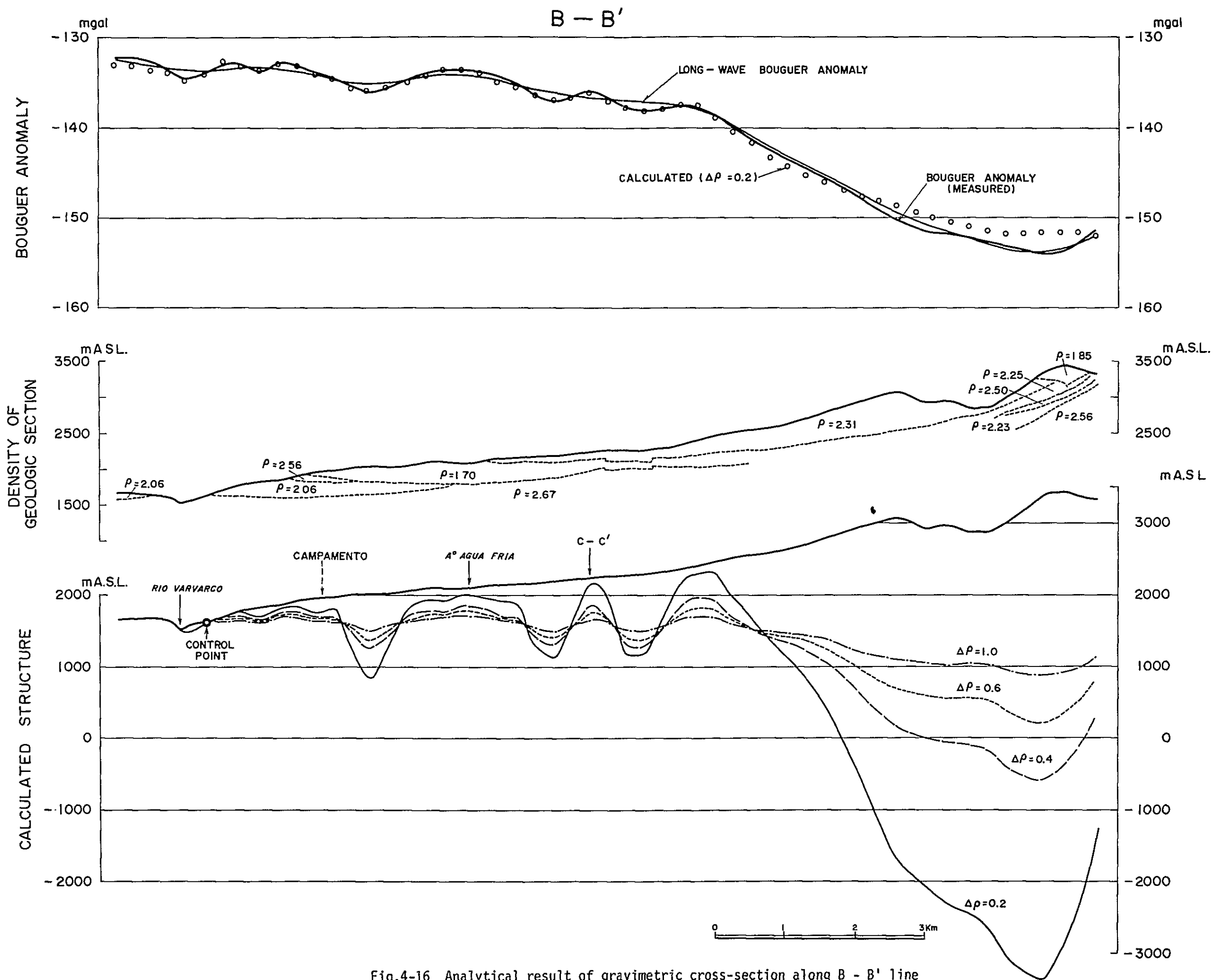


Fig.4-16 Analytical result of gravimetric cross-section along B - B' line

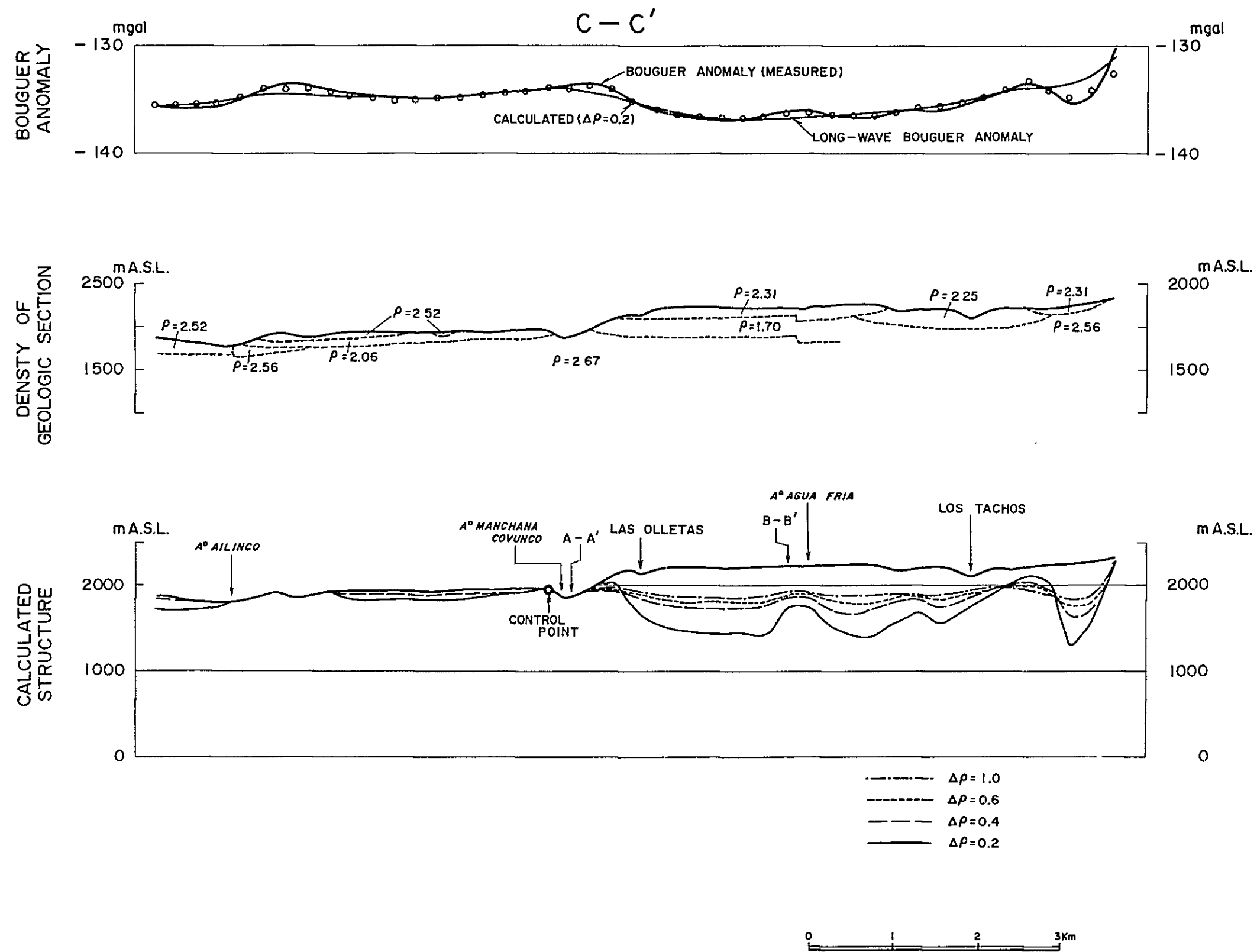


Fig.4-17 Analytical result of gravimetric cross-section along C - C' line

